Calhoun
Institutional Archive of the Naval Postgraduate School

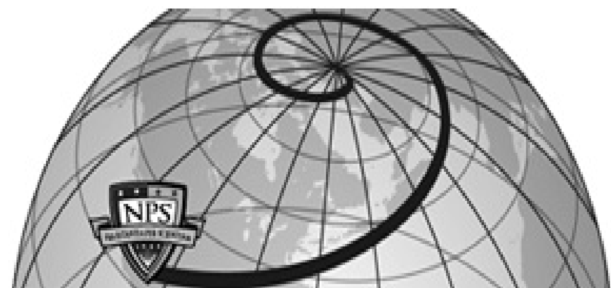

Calhoun: The NPS Institutional Archive

DSpace Repository

Theses and Dissertations | 1. Thesis and Dissertation Collection, all items

1966-05

Investigation of the Gunn effect in gallium arsenide

Slepicka, Alois Allen

Monterey, California. U.S. Naval Postgraduate School

https://hdl.handle.net/10945/9551

This publication is a work of the U.S. Government as defined in Title 17, United States Code, Section 101. Copyright protection is not available for this work in the United States.

Downloaded from NPS Archive: Calhoun

DUDLEY KNOX LIBRARY

Calhoun is the Naval Postgraduate School's public access digital repository for research materials and institutional publications created by the NPS community. Calhoun is named for Professor of Mathematics Guy K. Calhoun, NPS's first appointed -- and published -- scholarly author.

Dudley Knox Library / Naval Postgraduate School
411 Dyer Road / 1 University Circle
Monterey, California USA 93943

http://www.nps.edu/library

NPS ARCHIVE
1966
SLEPICKA, A.

INVESTIGATION OF THE GUNN EFFECT IN GALLIUM ARSENIDE

ALOIS ALLEN SLEPICKA

DUDLEY KNOX LIBRARY
NAVAL POSTGRADUATE SCHOOL
MONTEREY, CA 93943-5101

LIBRARY
NAVAL POSTGRADUATE SCHOOL
MONTEREY, CALIF. 93940

INVESTIGATION OF THE GUNN EFFECT
IN GALLIUM ARSENIDE

by

Alois Allen Slepicka
Major, United States Marine Corps
B.S., United States Naval Academy, 1954

Submitted in partial fulfillment
for the degree of

MASTER OF SCIENCE IN ENGINEERING ELECTRONICS

from the

UNITED STATES NAVAL POSTGRADUATE SCHOOL
May 1966

NPSARCHIVE
1966
SLEPICKA, A.
Thesis
S5

ABSTRACT

When the electric field in certain compound semiconductors exceeds a well-defined threshold value, the electrical current through the material becomes unstable. These instabilities may take the form of coherent oscillations at microwave frequencies. The oscillations are not greatly affected by external circuit conditions. The effect was first discovered in gallium arsenide and indium phosphide by J. B. Gunn in 1963, and is now referred to as the "Gunn effect". This paper discusses some of the practical aspects of the Gunn effect in gallium arsenide. A brief theoretical explanation is given, of the intervalley electron energy transfer mechanism which is now generally accepted as the mechanism through which the effect occurs. The preparation of samples is described, and the nature of the electrical contacts to the material discussed. Ohmic contacts are necessary to prevent junction effects or carrier injection from masking the oscillations. Mounting techniques are described. Circuit considerations are discussed, and the results of various measurements reported. The value of the Gunn effect lies in its potential to directly convert pulse or DC power into microwave power, at frequencies and power levels higher than is possible with other semiconductor devices, and at reasonable efficiencies.

LIBRARY
NAVAL POSTGRADUATE SCHOOL
MONTEREY, CALIF. 93940

DUDLEY KNOX LIBRARY
NAVAL POSTGRADUATE SCHOOL
MONTEREY, CA 93943-5101

TABLE OF CONTENTS

Section		Page
1.	Introduction	11
2.	Theoretical	14
3.	Preparation of Samples	26
4.	Sample Mounting	39
5.	Pulse Generators and Measurement Equipment	45
6.	Experimental Results	54
7.	Conclusions and Acknowledgements	64
8.	Bibliography	68

LIST OF TABLES

Table		Page
1.	Characteristics of GaAs Used	26
2.	Characteristics of Varian Gunn Oscillators	38
3.	Results of Contact Evaluation	54
4.	Diodes with Ohmic Contacts	55

LIST OF ILLUSTRATIONS

Figure		Page
1.	Characteristic Current-Voltage Relationship for Materials Displaying the Gunn Effect	11
2.	Electron Energy Band Structure Near the Bottom of the Conduction Band for n-type GaAs	15
3.	Current Density vs Electric Field for GaAs	19
4.	Spatial Carrier Density Distribution and Electric Field Distribution in an Oscillating Crystal	22
5.	Vacuum Chamber Used for Alloying Process	31
6.	Graphite Forms Used in the Alloying Process	33
7.	Diode Mounts	40
8.	Device for Current Waveform Measurements	42
9.	Coaxial Cavities	43
10.	Microwave Resonant Circuit	44
11.	Relay Pulser	46
12.	Thyratron Pulser	48
13.	Switching Diode Pulser	49
14.	Circuits for Measurements	51
15.	Current-Voltage Characteristics Observed	56
16.	Current Saturation	59
17.	Response to Thyratron Pulser	59
18.	Hysteresis Effect	60
19.	Coaxial Cavity Output for Diode 1026-5	61
20.	Instabilities in Varian Diode 90G3	63

TABLE OF SYMBOLS AND ABBREVIATIONS

C	capacitance
d	differential operator
E	energy
e	base of natural logarithms
F	electric field
f	frequency
J	current density
k	Boltzmann constant
N	effective density of state
n	charge carrier concentration
Q	quality factor of resonant circuit
q	magnitude of electronic charge
R	resistance
T	temperature
t	time
V	voltage
v	velocity
w	length of crystal
Δ	incremental quantity
ϵ	dielectric permittivity
μ	mobility of charge carriers
ρ	resistivity
σ	conductivity

Subscripts to the above symbols, when used, are self-explanatory or are explained in the text. Chemical symbols and units correspond to normal usage.

1. Introduction.

At the IEEE Conference on Electron Devices held in East Lansing, Michigan, in June, 1963; J. B. Gunn, of the International Business Machine Corporation, reported the observance of a new phenomenon in the bulk properties of certain compound semiconductors. [13] When placed in a strong electric field of a value exceeding some well-defined threshold value, the current through specimens of gallium arsenide (GaAs) and indium phosphide (InP) showed instabilities. In some samples, these instabilities took the form of coherent oscillations at frequencies in the microwave region. The phenomenon has subsequently been referred to as the "Gunn effect".

The Gunn effect is characterized by an ohmic current-voltage relationship in a sample, to within a few volts of some critical voltage, V_c; as shown in Figure 1. Beyond this value, the current no longer rises proportionately with voltage, and

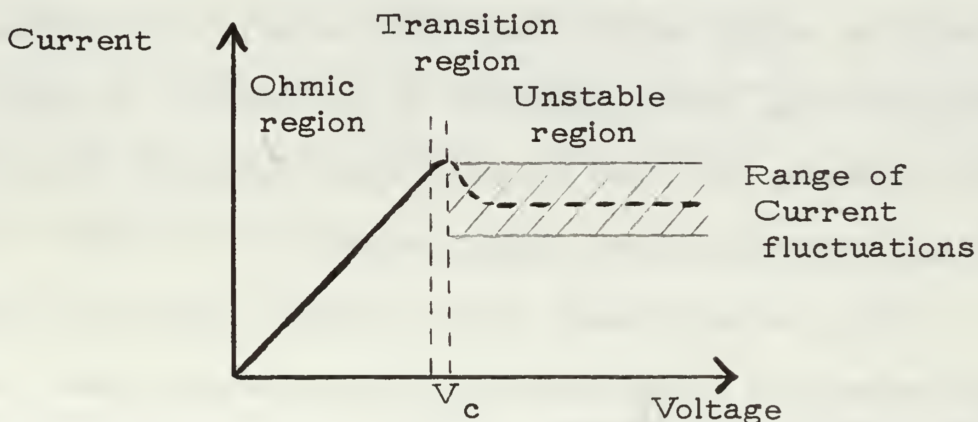

Figure 1 - Characteristic Current-Voltage Relationship for Materials Displaying the Gunn Effect.

beyond V_c, becomes unstable. In the unstable region, the average current remains constant or decreases somewhat with increasing voltage, as shown by the dotted portion of the curve in Figure 1.

The Gunn effect is a true bulk property of the materiels in which it occurs; in that, apart from the applied electric field (or voltage), no other special conditions of crystal orientation, preparation, or external environment (temperature, pressure, magnetic field, circuit, etc.) are necessary, except those required to prevent other effects from masking or swamping out the property. Non-injecting, ohmic contacts to the sample are necessary to prevent junction effects and/or carrier injection at the electrical contacts. Certain temperature limitations are imposed only to prevent destruction of the sample due to excessive heat induced mechanical stress, or to prevent excessive charge carrier generation. The effect can occur at any temperature, so long as the carrier concentration is within certain limits and remains at a reasonably constant level during operation of the device. In most materials displaying the Gunn effect, these conditions can be met at room temperatures and slightly above.

For a sample biased in the unstable region of Figure 1, the current is oscillatory with a period which shows some dependence on the width of the sample. The exact wave form depends on many factors discussed below, but consists of a

frequency spectrum in the microwave region.

At the time the effect was announced by Gunn, the exact causative mechanism was not known, although several explanations had been considered and rejected for various reasons. [18] The intervalley transfer of "hot" electrons, with a resulting internal negative differential resistance (described in Section 2), is now generally accepted as the explanation of the Gunn effect.[1]

The purpose of this project was to investigate the practical aspects of the Gunn effect. Gallium arsenide was selected as the material to be used. The preparation of samples, or diodes, from the bulk material was investigated in some detail and the results presented below. Suitable mountings for the diodes were considered, and various methods tried. Equipment for applying suitable fields without destroying the samples is discussed. Some items were especially constructed; and other commercially available equipment tried. Tests of the samples, both separately to determine the device characteristics, and as a circuit element, were carried out and the results reported below.

[1]Gunn had considered this explanation but rejected it as requiring too high an electron temperature (about 4000°K) from that experimentally observed (310°K - 400°K) [18]; but it was subsequently pointed out by Kroemer that certain assumptions made in arriving at the theoretical temperature were not valid for gallium arsenide. [24,26]

2. Theoretical.

With the invention of the tunnel diode, the negative resistance effects at semiconductor junctions attracted much attention and was the subject of intensive study. The next logical step was to inquire into the possibility of obtaining such an effect in a homogeneous material. As early as 1958, Kroemer (also spelled Krömer) proposed such a device by transferring some of the conduction band electrons to an energy level where they have a negative effective mass [3,5]. As reported by Hilsum, Burgess analyzed the situation based on carrier density as a function of electric field, and found it unpromising [10] . During 1961, Ridley and Watkins considered the possibility of arriving at negative resistance effects by utilizing other properties of the conduction band structure. They proposed the transfer of high mobility, low energy electrons in a subband of the conduction band to a low mobility, higher energy subband using materials with a suitable conduction band structure. They concluded their paper with the remark: "The existence of a negative resistance region in the current-voltage characteristic of a crystal may give rise to interesting effects due to electrical instability" [8] . It is now generally accepted that the Gunn effect is one of those "interesting effects" prophesied by Ridley and Watkins, and further explored by Hilsum in a later paper on transferred electron amplifiers and oscillators [10] .

The electron energy levels and band structure in GaAs are such that the conduction band consists of several subbands, or valleys, as shown in the simplified band structure diagram in Figure 2 [7]. Subband 1, at the bottom of the conduction band, contains most of the conduction band electrons in the relaxed state. The physical and electrical properties of the crystal usually specified are those associated with the electrons in this subband.

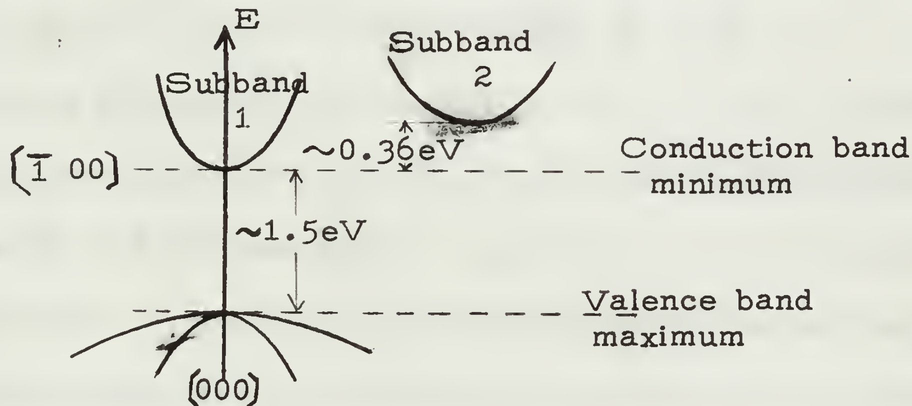

Figure 2 - Electron Energy Band Structure Near the Bottom of the Conduction Band for n-type GaAs.

Combining the effects of all satellite valleys[2] into subband 2; the conductivity, σ, of n-type material is given by [1]:

$$\sigma = q(\mu_1 n_1 + \mu_2 n_2) \tag{1}$$

[2]There is some question as to how many of these satellite valleys exist in GaAs. Ehrenreich [7] indicates there may be as many as six, as in silicon. Kroemer [40] agrees, if the valleys are inside the Brillouin zone; but points out that they may lie on the surfaces of the Brillouin zone. In this case they would be only half-valleys, and the effect would be that of three. Butcher and Fawcett [37], in their calculations, assume three.

where q is the magnitude of the electronic charge, μ_1 and μ_2 are the conduction electron mobilities for subband 1 and 2 respectively, and n_1 and n_2 are the respective electron concentrations for the two subbands. The usual assumption is made of conduction by electrons only, in n-type material, since the concentration of holes is negligible in comparison to electron concentration. The Boltzmann distribution law gives the equilibrium ratio of the number of carriers, n_1 and n_2, in each state at temperature, T, as [1] :

$$\frac{n_1}{n_2} = \frac{N_1}{N_2} e^{\frac{\Delta E}{kT}} \tag{2}$$

where N_1 and N_2 are the respective effective densities of state, ΔE is the energy difference between subbands, and k is the Boltzmann constant. The assumption is made that the total number of conduction band electrons, n , is constant and does not increase with an increase in the applied electric field, F. These conditions can be expressed as:

$$n = n_1 + n_2 \quad \text{and} \quad \frac{dn}{dF} = 0 \tag{3}$$

Combining (2) and (3), n_1 and n_2 are given as:

$$n_1 = \frac{N_1}{N_2} \frac{n e^{\frac{\Delta E}{kT}}}{\left(1 + \frac{N_1}{N_2} e^{\frac{\Delta E}{kT}}\right)} \tag{4}$$

$$n_2 = \frac{n}{\left(1 + \frac{N_1}{N_2} e^{\frac{\Delta E}{kT}}\right)} \tag{5}$$

The differential change in conductivity with electric field, F, is obtained by differentiation of (1) with respect to F, or:

$$\frac{d\sigma}{dF} = q\left(\mu_1 \frac{dn_1}{dF} + \mu_2 \frac{dn_2}{dF} + n_1 \frac{d\mu_1}{dF} + n_2 \frac{d\mu_2}{dF}\right) \tag{6}$$

Stratton has shown that mobility does not vary strongly with variations in applied electric field when energy transfer from a field to the crystal lattice is through optical mode scattering [4]. Ehrenreich indicates that polar optical mode scattering is the dominant scattering mechanism in GaAs [7]. This is also assumed to be the case by Butcher and Fawcett [37].[3] Thus, neglecting the latter two terms in equation (6), the expression reduces to:

$$\frac{d\sigma}{dF} = q\left(\mu_1 \frac{dn_1}{dF} + \mu_2 \frac{dn_2}{dF}\right) \qquad (7)$$

From (3), $\frac{dn_1}{dF}$ and $\frac{dn_2}{dF}$ can be related as:

$$\frac{dn_2}{dF} = -\frac{dn_1}{dF} \qquad (8)$$

Using (8), the expression in (7) can be further reduced to:

$$\frac{d\sigma}{dF} = q\left(\mu_1 - \mu_2\right)\frac{dn_1}{dF} \qquad (9)$$

Neglecting diffusion current, the current density J, and electric field are related by:

$$J = \sigma F \qquad (10)$$

Differentiation of (10) with respect to F results in the expression for differential conductivity:

$$\frac{dJ}{dF} = \sigma + F\frac{d\sigma}{dF} \qquad (11)$$

The condition for a negative differential conductivity is then:

$$\sigma + F\frac{d\sigma}{dF} < 0 \quad \text{or} \quad \frac{d\sigma}{dF} < -\frac{\sigma}{F} \qquad (12)$$

[3] The results are not particularly sensitive to the scattering mechanism. McCumber and Chynoweth report using several different two-valley models; all of which led to similar results [62].

Combining (9) and (12):[4]

$$g(\mu_2 - \mu_1)\frac{dn_1}{dF} > \frac{\sigma}{F} \tag{13}$$

This result shows that if a negative differential resistance is possible, it occurs over a range of values of electric field where the transfer of electrons to the upper subband, with increasing electric field, is sufficiently great to satisfy the inequality of (13). Stratton has arrived at a relation between the electron temperature, T, and electric field, F [4]. Hilsum has used this relation to plot a curve of current density versus electric field which shows a negative differential conductivity region beyond a critical electric field value, F_c, equal to about 3000 v/cm [10]. Using a more accurate model for electron temperature, Butcher and Fawcett arrive at essentially the same results, which are shown in Figure 3. They conclude that no significant intervalley transfer of electrons occurs until the critical field, F_c, is exceeded [37].

Only the static condition for the current density-electric field (or current-voltage) relationship is represented by Figure 3. As the critical field, F_c, is exceeded, the crystal becomes electrically unstable and this simple model no longer holds [8]. The mobility, μ, of the charge carriers is defined as [1]:

$$\mu = \frac{v_D}{F} \tag{14}$$

[4] Both $\frac{dn_1}{dF}$ and $(\mu_2 - \mu_1)$ are negative quantities.

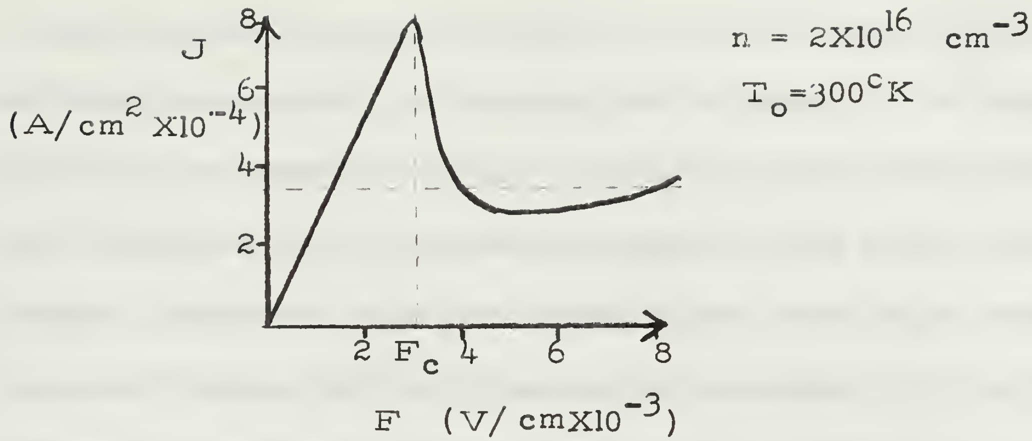

Figure 3. - Current Density vs Electric Field for GaAs. (After Butcher and Fawcett)

where v_D is the drift velocity of the carriers. Rewriting (14), the drift velocity is expressed as:

$$v_D = \mu F \tag{15}$$

In the two-valley model of the conduction band, the average drift velocity of the charge carriers is given by:

$$v_{D_{AV}} = \frac{n_1 v_{D_1} + n_2 v_{D_2}}{n_1 + n_2} = \frac{F}{n}\left(\mu_1 n_1 + \mu_2 n_2\right) \tag{16}$$

Current density, J , can be defined as:

$$J = q n v_{D_{AV}} \tag{17}$$

Thus, J and $v_{D_{AV}}$ differ only by a multiplicative constant. Figure 3, suitably scaled, applies also to $v_{D_{AV}}$, and a negative differential average drift velocity will also occur beyond the critical field value, F_c.

Within the crystal, any fluctuation in carrier density will produce a momentary space charge variation. The electric field within the crystal is then altered slightly. For a momentary increase in carrier concentration at some point in n-type material, the electric field increases slightly on the

positive electrode side of the space charge, and decreases slightly on the negative electrode side. Under positive differential conductivity conditions, this space charge is soon smoothed out by the slight increase in average drift velocity on the "downstream" side, and a slight decrease in average drift velocity on the "upstream" side, until the field again becomes uniform throughout the crystal. Under negative differential conductivity conditions, as when the electric field strength exceeds the critical value in GaAs, the momentary space charge does not dissipate. Instead, it builds up. The space charge will increase until the field strengths on either side of the space charge are high enough, and low enough, to equalize the current density on either side. In terms of the curve in Figure 3, this corresponds to high field and low field values along the positive-slope portions of the curve at the stable value of current density. This value of current density will be at or near the local minimum of the curve [41,46]. Electrical stability is thus restored in the crystal, but the field structure is very inhomogeneous. High field and low field "domains" are present, separated by a space charge layer.

The space charge layer is, of course, composed of charge carriers. Thus, it and the domains, will move through the crystal under the influence of the potential gradient between the contacts. Ridley has considered this domain mobility as just the effective mobility of the charges which can respond

to the applied electric field [14]. This value of mobility corresponds to the average electron drift velocity in the two domains after the space charge layer has fully developed and the velocity in the two domains equalized. In this case, the domain velocity is given by the equation for average drift velocity in (16) for the appropriate values of n_1, n_2, and F in the respective domains.[5]

As the space charge moves out of the crystal at the positive electrode, the field within the crystal is again in the negative differential conductivity region. The current density rises to its corresponding value for this field strength. A new space charge nucleates, and the domain formation process repeats. Thus, the current in the crystal oscillates between an upper and lower value.

Two explanations have been advanced for the nature of the space charge distribution resulting in the domain formation. Ridley proposed a dipole layer consisting of a charge accumulation layer followed by a charge depletion layer as indicated by the solid curve in Figure 4a [14]. A charge distribution of this type gives rise to the domain structure shown by the

[5] Kroemer has pointed out that for pure accumulation layers, this is not strictly correct, and that in the early stages of domain formation the accumulation layer propagates faster than the electrons comprising it [64]. However, the simplified Ridley model gives good results.

broken curve of Figure 4.a. Kroemer proposed a pure accumulation layer, as in Figure 4.b., in addition to the dipole layer [26,40].

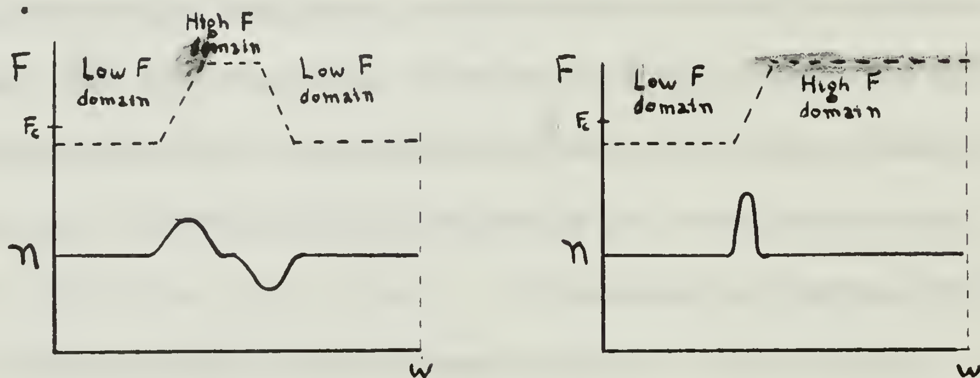

a. Dipole Layer (Ridley). b. Pure Accumulation Layer. (Kroemer)

Figure 4. - Spatial Carrier Density Distribution and Electric Field Distribution in an Oscillating Crystal (instantaneous in time).

Either type of domain structure will give rise to oscillations in the current through the crystal. The exact waveshape of the current fluctuations will be somewhat dependent on the type of domain structure from which they result. The pure accumulation layer requires a much more precise level of purity; hence, with presently obtainable levels of crystal purity (or controlled inpurities), the dipole structure is generally accepted as the dominant type actually observed experimentally.

The nucleation of the domain structure can occur wherever a fluctuation in carrier density is present. The domains will ordinarily form near the negative electrode, since the charge carriers enter at this point (in n-type material). Once the domain structure has fully formed, the crystal remains

stable until the space charge layer moves out of the crystal. A sharp variation in doping of the crystal near the negative electrode may be intentionally introduced to trigger the fluctuations. However, even in the absence of any noise fluctuations, or inhomogeneities in the crystal structure, the domains would still form due to the inevitable field gradient at the interface between the electrode and the crystal.

For idealized conditions, where the crystal is perfectly regular and the contacts geometrically planar and parallel, only one space charge layer exists at any time in the crystal. A new layer nucleates at the negative terminal, as the previous layer passes out of the crystal at the positive terminal. The oscillations are periodic, with a period equal to the length of time necessary for the layer to propagate through the crystal. For a crystal of length w , this corresponds to a frequency of oscillation, f, given by:

$$f = \frac{v_D}{w} \tag{18}$$

This is the expression for frequency of oscillation determined empirically by Gunn from his original experiments [18] .

In the usual case, the contacts are not perfectly planar, and the crystal is not perfectly regular. Successive domains may form at slightly different points in the crystal; and due to inhomogeneities, several may be present in the crystal at any given time. In extreme cases, no particular period can be associated with the instabilities. In this case, they have the

character of broad-band noise, and this is the usual case for long samples ($w > $ one mm). The instabilities in shorter samples are usually periodic, with complicated waveshapes [18] .

Sufficient charge carriers must be available in the crystal in order for the periodic formation of space charge layers to take place. Thus, below some critical value of carrier concentration, space charge layers cannot build up during the movement of a carrier through the crystal. Since carrier concentration in semiconductors is controlled by the amount of impurities present, below some critical doping level the oscillations will not occur. The time available for the space charge layer formation depends on the sample length. The produce of the charge carrier concentration, n , and the sample length, w , is used to specify this critical level. Using the Poisson equation, Kroemer has shown this relation to be [40] :

$$n = \frac{\epsilon}{q} \Delta F \tag{19}$$

where ΔF is the difference between the high and low fields of the domain structure, and ϵ is the dielectric permittivity of the material. Although ΔF has not yet been accurately determined, the value of the nw product in (19) has been experimentally observed to be on the order of 2×10^{10} cm^{-2} by Hakki and Knight [73] , and 7×10^{10} cm^{-2} by Day [72] .

The maximum frequency of oscillation is limited, in theory, only by the relaxation time for the transferred electrons from the higher to the lower energy state. Hilsum estimated the

upper frequency limit to be on the order of 10^{12} Hz [10]. This value is in agreement with the relaxation times between 10^{-12} sec and 10^{-13} sec recently calculated by Conwell and Vassell [63].

3. Preparation of Samples.

Six slices of single crystal, boat-grown, n-type gallium arsenide (GaAs) were obtained from the Monsanto Company, St. Louis, Missouri. Each slice had a thickness of about 20 mils (0.051 cm), and a density of 5.32. Characteristics of the individual slices, as supplied by Monsanto, are shown in Table 1. Slice numbers are the Monsanto ingot number. The first number in this sequence will be used subsequently in this report to indicate the origin of the various specimens. The slices varied in cross-sectional area from approximately two cm to about five cm, and were roughly semicircular in shape, typical of the boat-grown crystals.

Number	Doping	Carriers $cm^{-3} X 10^{-16}$ Front/Back	ρ-ohm-cm Front/Back	μ (25°C) cm^2/V-sec Front/Back	Wt. grams
55(162/165)	Undoped	1.00/.55	.39/.60	5000/4800	1.0
1026(28/51)	Undoped	1.3 /1.2	.12/.12	4100/4100	1.3
1137(170/216)	Undoped	.85/.79	.16/.20	4400/4000	0.6
214(158/205)	Oxygen	.75/.58	.18/.24	4800/4500	1.2
276(59/70)	Oxygen	.053/.087	2.2/1.4	5700/5400	0.6
1162(216/258)	Oxygen	.28/.11	.54/1.2	4600/5200	1.2

Table 1 - Characteristics of GaAs Used.

Specimens were prepared by cutting strips approximately two mm in width, from each slice. Each strip was then cut into squares (two mm). A slow speed, motor driven wire

saw, charged with a silicon carbide abrasive, was used for cutting this frangible material. A very fine, single strand Chromel wire was first tried, but proved to be unsatisfactory. Sufficient tension on the wire could not be obtained (without breaking the wire) to force the abrasive against the slice. Using moderate tension, a sawing time of about 96 hours produced only a shallow groove in the material.

A single strand, #28 nichrome wire was next tried, and produced satisfactory results. An average cutting time of five hours was required to cut through the 20 mil thickness of the slice. The finest silicon carbide grit on hand (#600) was used to charge the wire. The grit was suspended in silicone diffusion pump fluid (Dow Corning 704 fluid). A small trough of molding clay (which was also used to hold the slice while sawing) was formed on the slice along the line of cut of the saw. The silicon carbide, suspended in the silicone oil, was placed in the trough and kept the wire continuously charged and lubricated during the sawing operation.

Examination of the GaAs edges after sawing, showed that the wire had not actually cut all the way through the slice. After sawing through about three-fourths of the thickness, the crystal fractured along the line of the saw cut. For the subsequent sawing operations of cutting the strips into squares, this fact was used to speed the operation, and to make the handling of the small squares somewhat more

convenient. The strips were sawed through only about two-thirds of the thickness, and the individual squares separated from the strip as needed, by tapping lightly at the saw cut. In every case the material fractured along the cut. This produced rough edges; however, the edges could be smoothed by lapping, as described below.

Speed of the wire across the slice during the cutting operation averaged about 0.4 cm/sec (the motion of the wire was back-and-forth, with the instantaneous velocity of the wire following a sine curve). The speed (average) of the wire was adjustable, but no other setting was tried, since satisfactory results were obtained with the above indicated speed.

After sawing into squares, the specimens were cleaned in tricloroethylene, then lapped to the desired thickness. Lapping was done by hand on a small, stainless steel lapping table. To hold the specimen while lapping, it was cemented to a flat piece of cork using ordinary fast-drying mending cement. After lapping, the cement was dissolved in acetone to free the specimen. Silicon carbide (#600 grit) and powdered alumina suspended in water were used as lapping agents. Using this method, thicknesses less than about 0.2 mm could not be achieved without fracturing the specimen. The cross-sectional area could be reduced, and the edges smoothed, by lapping the edges of the specimen. Extreme care was necessary while

performing this operation, to prevent chipping along the sharp edges. After lapping, the specimens were cleaned in tricloroethylene, etched in an acid-peroxide etchant[6], and chemically polished in a 0.05 per cent (by volume) solution of bromine in methanol. After polishing, the specimens were rinsed in a five per cent (by weight) solution of potassium cyanide (KCN) to remove any contaminating copper. Finally, an ethanol rinse was used to remove any water from the specimens; after which they were dried in air.

As mentioned in Section 1, non-injecting, ohmic contacts must be applied to a specimen in order to observe the instabilities due to the electron transfer mechanism. A variety of methods and materials have been used to apply electrical contacts to GaAs [16,17,18,21,73] .

The suitability of a material depends on its effect on the GaAs. Alloyed contacts of indium (In), tin (Sn), or indium-gold (In-Au), have been most widely used.[7]

Pressure contacts using indium and tin were first tried,

[6] Two etching solutions were tried. The first consisted of three parts (by volume) H_2SO_4, one part H_2O_2 (30% solution), and one part H_2O. The second consisted of one part HF, one part H_2O_2 (30%), and two parts H_2O. The sulphuric acid etch produced the faster etching action, but the HF etch produced more even etching over the specimen.

[7] See also [6] , pages 25-67, for a discussion of the effects of the diffusion of various impurities into GaAs. Many other papers listed in the bibliography include a paragraph or more on the method used to apply contacts to GaAs.

but are not particularly good due to the frangible nature of the specimens. Tin squares, 0.1 mm thick, cut to the size of the specimen, were etched in a solution of one part (by volume) HNO_3 to one part H_2O; then in a solution of one part (by volume) HCl to one part H_2O; rinsed in distilled water, and dried. Indium discs, approximately 0.5 mm in width, were cut from one mm diameter indium wire; polished in the 0.05 per cent bromine in methanol solution as for the GaAs; rinsed in ethanol and dried. The contact material was placed in position on the GaAs specimen, and held in place by the mounts described in Section 4.

The indium, being very soft, showed a tendency to adhere well to metallic surfaces against which it was pressed. Since tin does not adhere in this manner, some tin contacts were made by taking a small dot of indium and spreading it over the GaAs surface to which the tin contact was to be applied. The tin was then pressed against the surface, and the very thin layer of indium held the tin in contact with the GaAs.

Indium produced the better physical contact, as indicated above, but crept, under pressure, around the edges of the specimen. Eventually, an electrical short circuit across the specimen was produced. These diodes could be restored by trimming away the excess indium, but in almost all cases the specimen eventually fractured.

Attempts were made to produce alloyed contacts of tin to the GaAs. A vacuum chamber was constructed for the alloying process. Machined brass end plates closed a six-inch length of one-inch diameter Pyrex tube. One end plate carried the vacuum fitting; while the other was fitted with a glass-to-metal vacuum seal with two electrical leads used to connect a thermocouple for monitoring temperature. Double, rubber O-ring seals were used in each end plate for the vacuum seal. A Hastings Ion Vacuum Gauge, Model GV-3, was placed in the vacuum line to monitor the system pressure. A sketch of the vacuum chamber is shown in Figure 5.

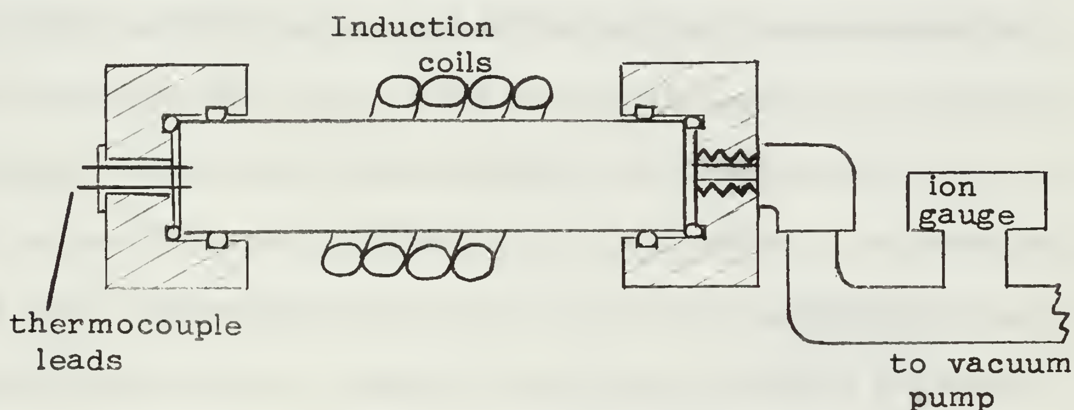

Figure 5. - Vacuum Chamber Used for Alloying Process.

A Duo-Seal vacuum pump, powered by a one-half horsepower AC motor, was used to evacuate the chamber. The highest vacuum recorded with this system was $1.8X10^{-2}$ Torr (mm of Hg) as measured by the vacuum gauge. This was achieved after a pumping time of about one and a half hours. Continued pumping for about 15 minutes produced no discernible decrease in pressure. Usual values of vacuum achieved were

on the order of 0.1 - 0.2 Torr. Values in this range were reached after about 30 minutes of pumping. In each case that the chamber was evacuated, the induction heater was not activated until no discernible change had occurred in the vacuum reading for at least five minutes.

A Toccotron (Ohio Crankshaft Company), type 1EG11-1, induction heater was used to provide the heat necessary for the alloying process. Four turns of one-quarter inch copper tubing was used for the induction coil. The inside diameter of this coil was made just slightly greater than the outside diameter of the one-inch Pyrex tube. The temperature of the thermocouple tip, placed at the center of the coil (along the axis), remained steady at 620°C with the induction field on. The induction pulse could be varied from five seconds to 60 seconds. Frequency of the induction current was 450 KH_z. The thermocouple used was of iron and constantan, with a total resistance (including leads) of 16 ohms. It was used with a thermocouple millivoltmeter. The voltage readings were converted to temperature by a standard table of conversions for iron-constantan thermocouples.[8]

To hold the contact and specimen in position during the

[8] Although the millivolt meter was calibrated for a thermocouple resistance of 4.03 ohms (chromel-alumel), and the thermocouple used had a resistance of 16 ohms, this introduced a negligible error due to the high internal impedance of the meter. The meter also had a scale which would read temperature directly for a chromel-alumel thermocouple.

alloying process; and to provide sufficient hydrostatic pressure, graphite forms were constructed. The hydrostatic pressure is necessary to keep the molten tin in contact with the specimen during the alloying process. Without the pressure, the surface tension of the molten tin causes it to assume a spherical shape with only a small area actually in contact with the specimen.

One type of form used consisted of a cylindrical, flat-bottomed cup of graphite, into which was inserted a loose-fitting, cylindrical graphite plug, as in Figure 6.a. The second type used was similar, but rectangular in shape with open ends, as shown in Figure 6.b. In either case, several specimens

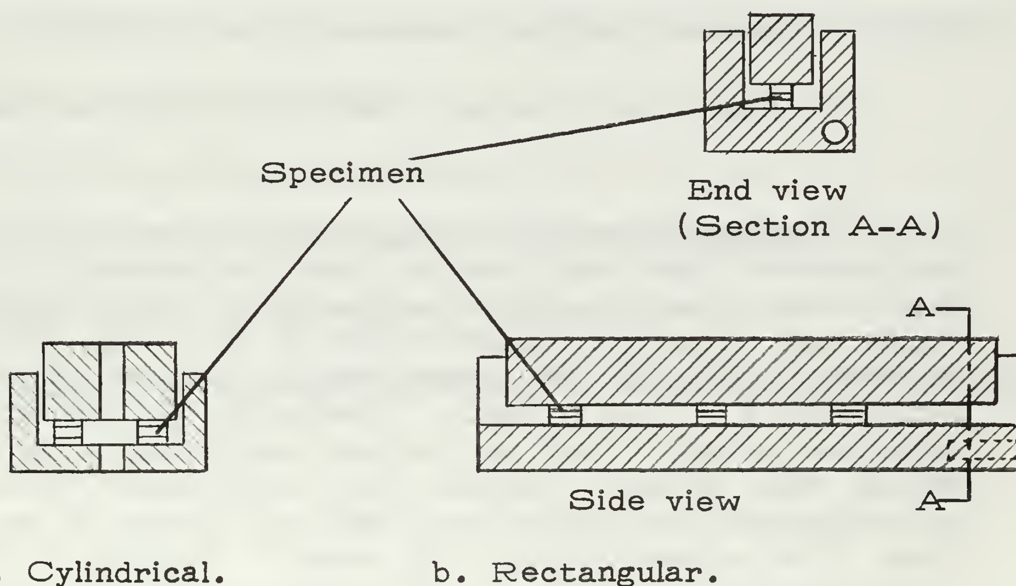

Figure 6. - Graphite Forms Used in the Alloying Process, (About twice actual size. Specimens not to scale)

could be inserted at a time, as shown. At least two at a time were necessary to keep the plug face parallel with the surface on which the specimens were placed. In the cylindrical form, the thermocouple was inserted in the center hole. In the rectangular form, a small hole was drilled in the base, as shown in Figure 7.b., and the thermocouple tip inserted. The tip of the thermocouple was thicker than the tin-GaAs combination, hence it could not be inserted under the graphite plug with the specimens.

Prior to attempting the actual alloying, the graphite was first heated to a high temperature in the vacuum chamber, to remove possible contaminants in the graphite. Several runs were then made with tin alone to determine, by observation, the thermocouple reading at which the tin in contact with the graphite melted. Temperature of the graphite, after 30 seconds of induction heating, measured about 500°C.[9]

For the actual alloying, the GaAs specimen was placed

[9]Metals imbedded in the graphite absorb RF energy from the induction field much better than the graphite. Thus, the thermocouple reads a higher temperature (that of the thermocouple tip) when the inductive field is on. Only after the field is turned off, does the thermocouple accurately indicate the temperature of the graphite. Similarly, the tin will melt, with the inductive field on, before the graphite heats to the melting point of tin. Ideally, the thermocouple tip should be placed against the GaAs; but this, of course, is not practical. The temperature of the graphite apparently follows a curve of the form $(1 - e^{-t})$ while heating and (e^{-t}) while cooling [92] .

between two flat tin contacts, and the combination placed in the graphite form, as shown in Figure 6. The temperature was kept between 400°C and 500°C by manually operating the induction heater. Various alloying times were tried, from 30 seconds to five minutes. Upon completion of the application of heat, vacuum pumping was continued until the graphite had cooled to approximately room temperature. At this time, the vacuum chamber was opened, and the specimen removed.

The attempts at alloying were not successful. After most runs, examination of the specimen and contact which were still separate, showed that the tin had failed to "wet" onto the GaAs. In some cases, the tin was no longer bright, but had acquired a film. No analysis was made to determine the nature of this film. In those cases where the tin had appeared to adhere to the GaAs, subsequent handling soon separated them. The lack of success with the alloying process is attributed to three factors:

(1) Insufficient vacuum.

(2) Difficulty in maintaining accurate temperature adjustment using the procedure outlined above.

(3) Impurities present in the apparatus; particularly in the graphite.

The successful alloying processes described in the literature usually use an atmosphere (at reduced pressure) of purified hydrogen. A method for obtaining high purity hydrogen

is contained in reference [9].[10] No attempt was made to introduce a forming atmosphere into the vacuum chamber during the various alloying runs. In those cases where a high vacuum has been used, pressures of 10^{-4} Torr to 10^{-5} Torr have been reported [17].

Alloying temperatures must be kept below about 600°C. Above this temperature, significant dissociation of the GaAs occurs, and impurities are rapidly diffused into the material [17]. In the presence of water vapor, an oxide film forms on the GaAs during alloying, which interferes with the alloying process [18]. An oxide film can also form on the GaAs if the time between the chemical cleaning and etching process, and the heat treatment, is longer than a few minutes [92].

An anhydrous hydrocloric acid bath for both the specimen and the contacts immediately prior to the start of the vacuum pumping was tried. This was done in an attempt to achieve an HCl atmosphere (at the vacuum pressure) for the alloying operation. An HCl atmosphere has been reported, in some cases, to promote the alloying process [92]. The specimen and contacts were dipped into the HCl and immediately placed into the graphite form without drying. No significant improvement was noted in the results, when adding this step to the

[10] See [9], pages 112-118. This reference also contains a discussion of vacuum techniques, in addition to other useful information.

alloying procedure.

Hydrazine dihydrochloride was tried as a wetting agent on two runs, without improvement in the results [26]. The action of the hydrazine dihydrochloride, when tried during a test run with a strip of copper[11], was identical to that of a similar test run with HCl. The tin soldered evenly over the copper; the hydrazine dihydrochloride (and HCl) acting as a flux to clean the copper and destroy the surface tension of the molten tin.

The presence of lead (Pb) does not appear to have a deleterious effect on the electrical properties of the GaAs or the contact junction.[12] Ordinary 50-50 tin-lead solder was tried as a contact material during two alloying runs. One run was made with resin flux in the solder; the other with the pure alloy. In neither case was any improvement noted in the results. Pressure contacts of 50-50 solder exhibited the same properties as pure tin pressure contacts.

Pressure contacts of pure aluminum were tried, but good contact could not be made with the GaAs without fracturing the specimen. The use of no contact material was also tried on one specimen. The GaAs was placed between

[11] To prevent contamination by the copper, a different piece of graphite was used, from that used with GaAs. Also, no plug was used. The copper was placed on a strip of graphite, with the tin contact placed on it without pressure.

[12] See [6], pages 25-67.

two brass relay contacts. The electrical response was strongly non-ohmic.

Two diodes with alloyed tin contacts were supplied by Dr. D. G. Dow, of Varian Associates, Palo Alto, California. The characteristics of these devices are shown in Table 2.

Device	Size mil	w micron	R - ohms		Threshold Voltage		Threshold Current		Power watts		f - MHz	
			Pos	Neg	Pos	Neg	Pos	Neg	Pos	Neg	Pos	Neg
90B7	40X40	80	2.5		24		8.0	7.5	12	23	1030	800
90G3	40X40	80	2.5	2.4	22	28	6.5	8.0	36	11	660	1060

Table 2. - Characteristics of Varian Gunn Oscillators.

4. Sample Mounting.

For the various tests performed on the diodes, several mounting methods were used.

The first mount tried was constructed from a thin strip of printed circuit board about six cm long and 0.24 cm thick. Four small brass nuts were soldered, in-line, to the board, and the copper removed between the inner two nuts on both the upper and lower surface of the board. Two brass bolts placed through the nuts, held the diode in place as indicated in Figure 7.a. This mount could be placed as a section of the inner conductor of 50-ohm, air dielectric, coaxial transmission line, for high frequency tests. For low frequency measurements of the diode characteristics, it could be used alone. The layer of copper to which the nuts were soldered was thin. This allowed some movement of the nuts, which posed alignment problems, and problems of keeping the diode in place without damaging it.

A more suitable holder of the same general type was made by threading the inside of a short length of one-fourth inch rigid plastic tubing. A slot was cut into the center of the tube. Tinned brass bolts were screwed into both ends, and held the diode in place at the center slot as shown in Figure 7.b. This mount could also be inserted along the inner conductor of a coaxial line. It was also difficult, with this mount, to keep the bolts tightly in place, thus insuring proper

a. Printed-Circuit Board Mount.
(Actual size)

b. Plastic Tube Mount.
(Twice actual size)

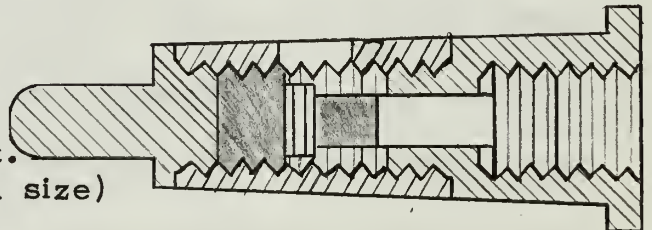

c. Radar Diode Mount.
(Four times actual size)

Figure 7. - Diode Mounts.

contact with the diode.

Several coaxial holders for radar diodes, which were readily available, prompted the use of radar diode mounts for mounting the GaAs diodes. Several discarded 1N21 diodes were disassembled, and the semiconductor material removed from the shaft of the screw. This shaft was then extended about 0.5 cm with a column of solder. The base of the mount was filled with solder to the level of the small hole in the ceramic body of the diode. The GaAs diode was held in position between the screw shaft and the base, as shown in Figure 7.c. This mount proved to be satisfactory in all respects.

A device similar to that used by Gunn for current waveform measurements, was constructed [18]. This mount allowed simultaneous connections to a spectrum analyzer and oscilloscope sampling unit, for analysis of the applied voltage and resulting current through the diode. Either mounted or unmounted diodes could be used with this device. The device was made from copper plates and two relay contact arms, as shown in Figure 8.a. Two coaxial terminals were attached to each side. The two inner conductors on each side held the contact arms in position, and the tension of the arms held the diode in place between the arms. Resistance could be inserted between each arm and the body of the device as shown. The equivalent circuit is shown in Figure 8.b. The resistance, R_1, is selected to be of the same order of magnitude as, and less than the diode impedance. The resistance, R_2, is a current sampling resistance, a small fraction of the value of the diode resistance.

For power measurements, a coaxial cavity was constructed. The diode was mounted in series with the inner conductor. Both ends of the cavity were closed (one-half wavelength resonator). One end was insulated from the outer conductor, which allowed the input pulse to be applied across the diode by connections to the outer conductor and this fixed end piece. The other end piece was movable, for varying the cavity length. The inner conductor could be moved independently of the end

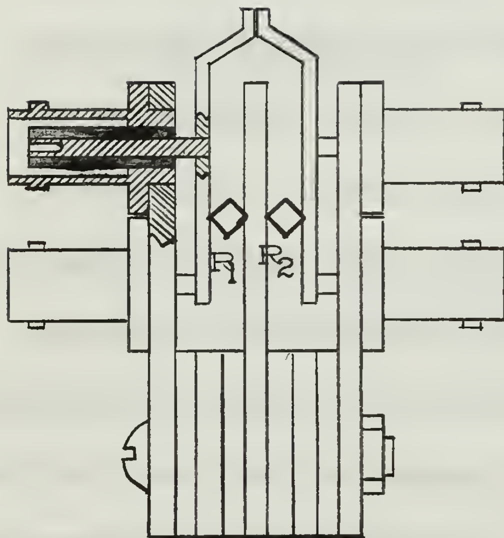

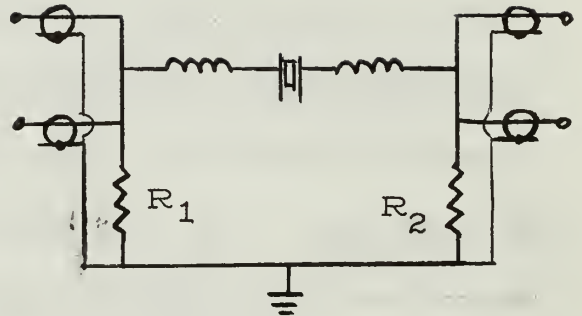

a. Device. b. Equivalent Circuit.

Figure 8. - Device for Current Waveform Measurement.

pieces, which allowed the position of the diode within the cavity to be varied. Capacitance between the fixed end piece and the outer conductor was sufficient to act as a low impedance at microwave frequencies. This capacitance could be varied by varying the depth of penetration of the end piece into the cavity. Coupling to the cavity was by means of a loop or probe inserted through small holes drilled along the length of the outer conductor. A sketch of the cavity is shown in Figure 9. The very high quality factor (Q) for this cavity (∼4000), and the lack of a precision tuning mechanism caused difficulties in making measurements. For this

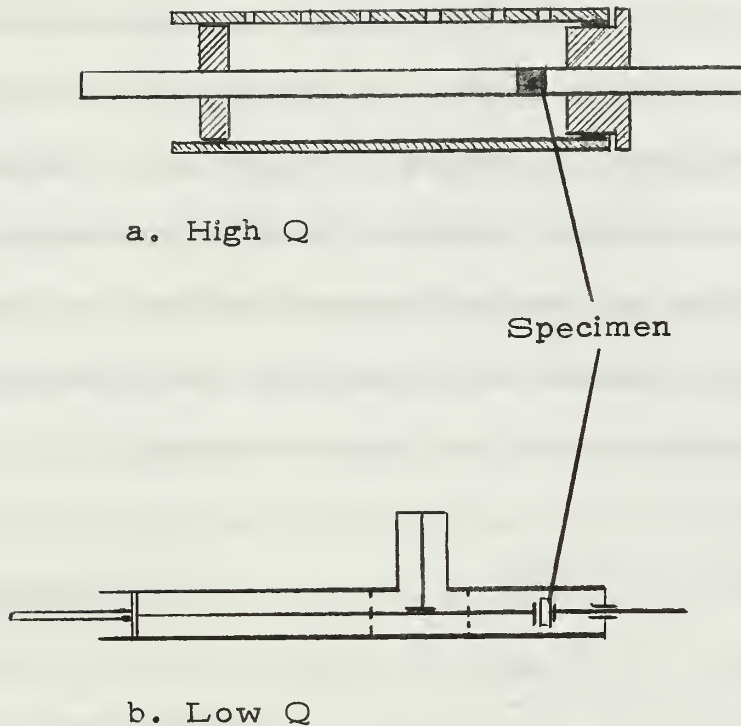

Figure 9. - Coaxial cavities.

reason, a coaxial cavity resonator was also constructed from sections of General Radio 50-ohm, air dielectric, one-inch diameter, transmission line and associated hardware. Cavity lengths could be adjusted using an adjustable "short" section. Coupling was by means of standard hardware modified as the needs required. A sketch is shown in Figure 9.b.

The Gunn diodes supplied by Dr. Dow of Varian Associates, were mounted on the flat end of a tinned brass bolt. These diodes were used with a mount similar to Figure 7.b. In place of a second bolt, however, the base of a 1N21 radar diode (Figure 7.c.) was used. The device could then be inserted in the radar diode holder used with the resonator in

Figure 9.b.

A microwave resonant circuit was also constructed for use with the Varian diodes. A sketch, with the equivalent circuit (simplified), is shown in Figure 10. The capacitive coupling to the output could be varied by increasing or decreasing the amount of overlap between the two conducting surfaces, one in contact with the diode, the other connected to the inner conductor of the output terminal.

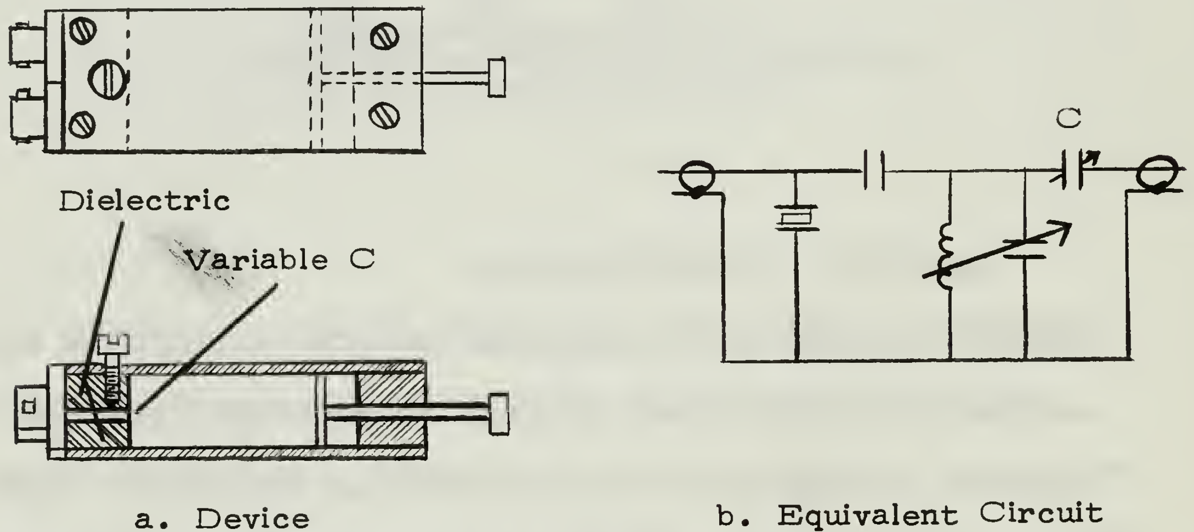

Figure 10. - Microwave Resonant Circuit.

5. Pulse Generators and Measurement Equipment.

After assembly and mounting of the diodes, the first measurements were directed toward determining the nature of the contacts, and the DC resistance of the diode.

For a diode with ohmic contacts, a very low resistance is expected. A sample thickness of 0.15 mm, a cross-sectional area of about four mm^2, and a resistivity of one ohm-cm, produces a sample resistance of less than one ohm. A device with the above thickness, in which an electric field strength of several thousand volts per cm is to be produced, requires a potential difference between contacts on the order of tens of volts. A current flow through the device, in amperes, of the same order of magnitude as the voltage (up to the critical voltage, V_c) results. To prevent damage to the diode, and thermal generation of charge carriers, pulses of very short duration are required. For the Gunn effect to be observed, the voltage must remain in the negative differential resistance region for a significant portion of the pulse length. Thus, high power, short duration, fast rise-time pulses are required for pulsing low resistance Gunn diodes.

A General Radio 1217B pulse generator was initially tried, with 0.1-0.5 μsec duration pulses at a low repetition rate (usually 100 pps). Those diodes displaying a resistance higher than one kilohm, were further tested with a DC voltage supply with current limiting (Hewlett-Packard 721A Transistor

Power Supply). The 1217B pulse generator was not satisfactory for pulsing a low impedance load. The internal impedance of the generator was too high to deliver pulses of an amplitude of more than a few volts to a low impedance load. The internal impedance varied with output, and at maximum output was about one kilohm.

To produce a pulse which would maintain a high voltage across a low impedance, a simple capacitor discharge circuit was assembled. The circuit is shown in Figure 11.a. The mechanical relay was either operated by hand or pulsed by the 1217B pulse generator. The circuit produces the well-known exponential pulse, whose decay rate is varied by varying R_1. The value of the resistor, R_1, which is the same as that in Figure 8, was selected to be less than the diode resistance.

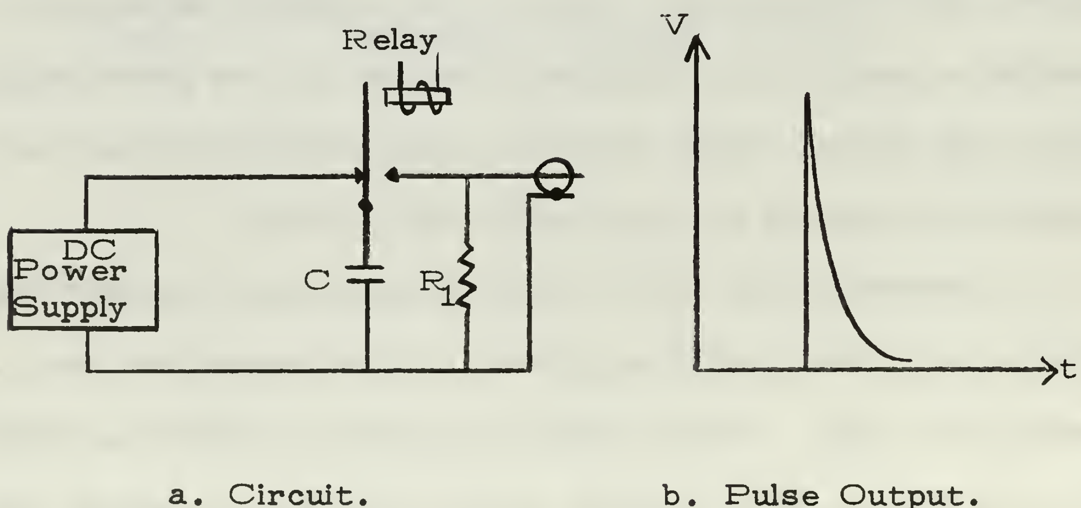

a. Circuit. b. Pulse Output.

Figure 11. - Relay Pulser.

Typical values of capacitance used varied from 0.5 to 8.0 μf. Values of R_1 varied from 1.4 to 100 ohms. This circuit was abandoned due to arcing at the relay contacts above about 15 volts, and excessive "bounce" of the contacts on closing.

The same basic idea was again tried, with a thyratron replacing the relay. The circuit is shown in Figure 12.a. A CW-394A thyratron was used, which fired at a grid voltage of minus five volts. The thyratron could be turned off by applying a high negative voltage (-30 v) to the grid. Various values of C and R_1 were tried. For R_1 of 2.7 ohms and C of 0.001 μf, the pulse shown in Figure 14.b. was observed at the output. The pulse duration was observed as 80 nsec. The pulse shape and duration may have been due to the response limitations of the oscilloscope used (Tektronix 515A; rise time: ~20 nsec; frequency response: ~10 MHz). Unless the grid trigger input amplitude was carefully adjusted, the output sometimes consisted of two pulses separated by a time interval of the order of a few hundred nsec. This occurred due to a change in voltage drop across the thyratron as the grid voltage changed from a negative to a positive value (or zero). As the increasing grid voltage reached minus five volts, the voltage drop across the thyratron dropped from V_b to about 100 volts. As the grid became positive, the voltage across the tube dropped to about 30 volts. By adjusting the amplitude of the trigger pulse to such a value that

the grid remained negative, the second pulse was eliminated. Pulse repetition rates no greater than one pulse per millisecond were used. For these rates, deionization time of the thyratron presented no problems, and was not measured.

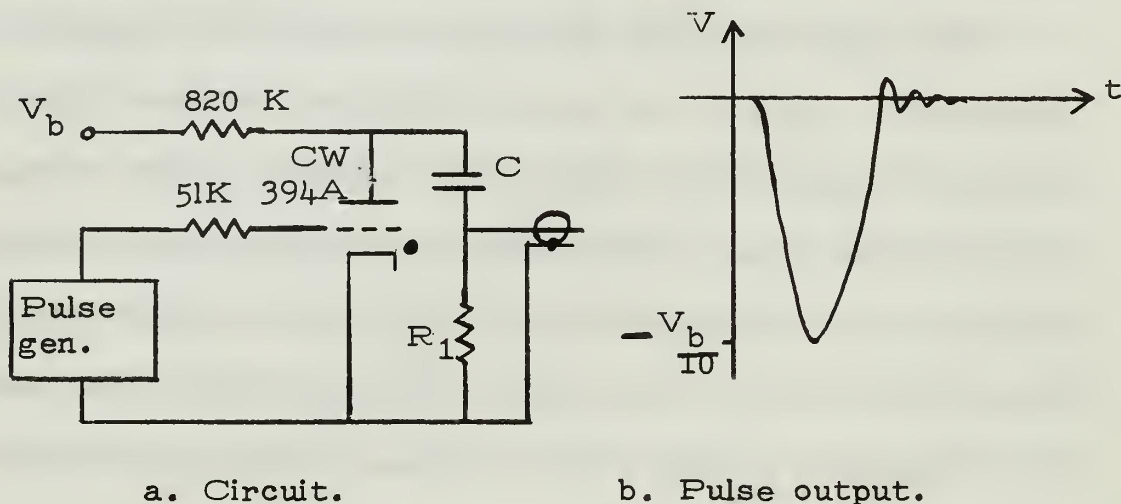

a. Circuit. b. Pulse output.

Figure 12. - Thyratron Pulser.

In an attempt to achieve a faster pulse rise time, a switching diode, 2N687, was tried. The circuit is shown in Figure 13.a. For the low values of C and R_1 used, the switching diode was not able to switch fast enough to produce a sharp pulse. The plot in Figure 13.b. shows the voltage across the switching diode as a function of time, for the best combination of gate-pulse amplitude (50 v from a bias level of -35 v), and V_b (200 v). The turn-off time for this combination was about 30 μsec. Since a satisfactory pulse generator became available, faster semiconductor switching devices were not explored.

A Dumont 404B pulse generator was also investigated. This device has an internal impedance of 50 ohms for matching

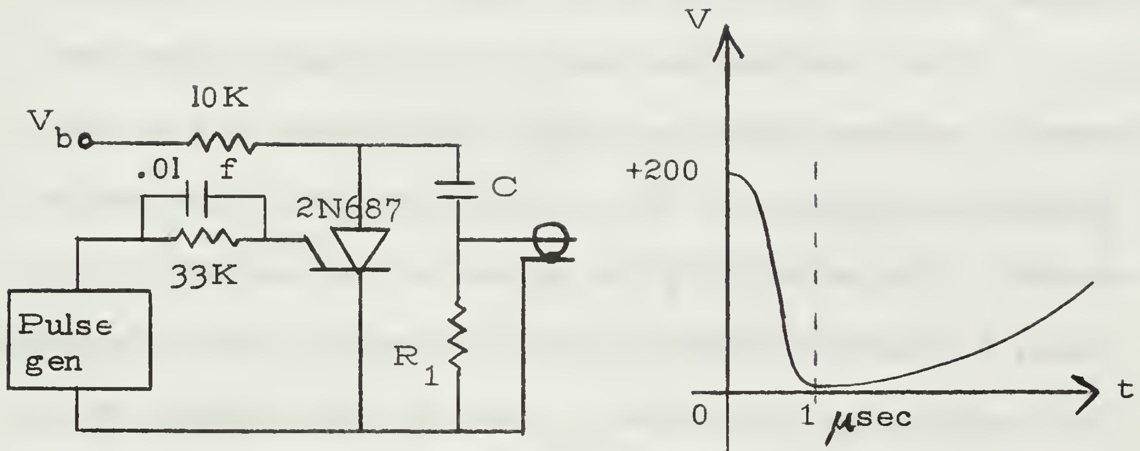

a. Circuit. b. Switching Characteristics.

Figure 13. - Switching Diode Pulser.

to 50-ohm coaxial transmission lines. Maximum pulse amplitude is about 100 volts. Pulse rise time is about 50 nsec. The principal disadvantage of this device is "ringing" of the pulse, which becomes excessive for load impedances below 50 ohms.

The most satisfactory pulser used was an SKL Model 503 Fast-Rise Pulse Generator. This device generates a fast rise-time square pulse by discharging a length of charged transmission line through a relay with mercury-wetted contacts. Pulse repetition rates of up to about 200 pps were obtainable. Pulse amplitude was continuously variable from -150 v to +150 v. Pulse lengths could be varied by adjusting the length of transmission line used. Polyethylene dielectric, 50-ohm coaxial

lines were used, which produce a pulse length of about one nsec per eight inches of line.

To observe the effects of the pulses applied to the diodes, several methods were employed.

A direct oscilloscope display of the longer pulses was possible, although the fine details were lacking due to the band-pass limitations of the internal circuits of the oscilloscopes. For determining the nature of the contact to the GaAs, a Hewlett Packard Model 122A and a Tektronix Model 515A oscilloscope were used. Both of these devices have a frequency limitation of about 10 MHz maximum, and a minimum rise time of about 20 nsec. Hence, only average values of current could be displayed. Instabilities could be indirectly detected by deformation of the input pulse and, at times, by "jitter" in the output pulse. An output proportional to the current through the diode was obtained by the small resistor, R_2, of a value of about one-tenth the diode resistance, placed in series with the diode. The circuit is shown in Figure 14.a, and was used with the device in Figure 8.

For direct observation of the details of the current instabilities, a Tektronix Type N Sampling Plug-in Unit, used with the Tektronix 535 oscilloscope, a Type 111 Pretrigger-Pulse generator, and a CBTV-P6025 capacitive probe, were used. This combination takes one sample of each pulse; which is recorded as a single spot on the oscilloscope. The sampling

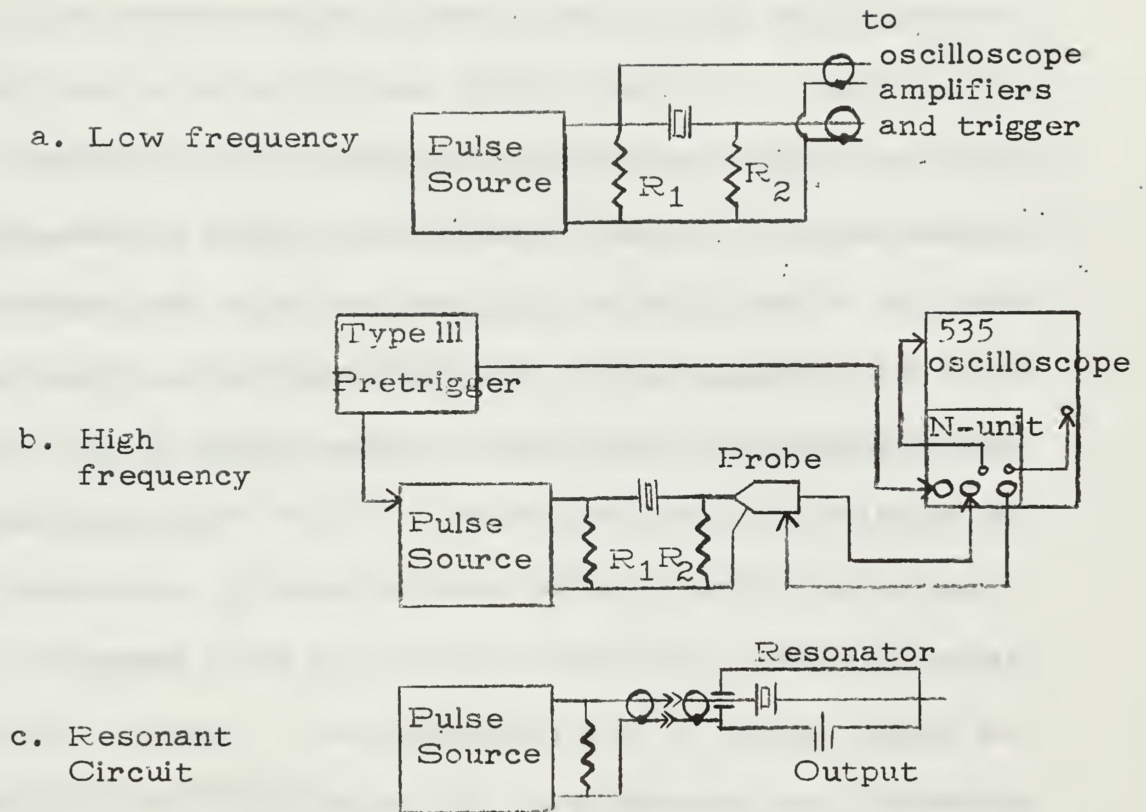

Figure 14. - Circuits for Measurements.

point on the pulse, and the horizontal position of the oscilloscope display, is advanced a small, predetermined amount for each successive pulse. In this manner, a periodic waveform can be displayed, whose frequency exceeds the band-pass limitations of the oscilloscope. The pretrigger unit provides the synchronization necessary among the sampling units, the pulse source, and the oscilloscope. The circuit diagram is indicated in Figure 14.b.

The Type N sampling unit developed a 60-cycle ripple, superimposed on the output trace, which prevented an accurate display of the sampled waveform. An attempt was made to employ the fast rise-time and sampling properties of a Hewlett

Packard Model 1415A Time Domain Reflectometer with Model 140A Display. A circuit similar to Figure 14.a. was used, with the output connected to the signal input terminal of the reflectometer. R_2 was replaced by a simple voltage divider, with the output at about one volt, to meet the requirement for a low voltage input to the reflectometer. Synchronization was attempted by triggering the pulse generator with the output signal of the reflectometer, but this was unsuccessful. A degree of synchronization was achieved by continuously adjusting the pulse repetition rate of the pulse generator and the display sweep of the reflectometer. Noise in the system prevented the observance of the instabilities due to the GaAs diodes. A square pulse, with a ragged top, was observed, but the top remained ragged when the GaAs diode was replaced by an equivalent resistance. No change in the appearance of the trace was noticeable when this was done.

Frequency measurements were made by a Polrad Model SA-84WA Wide Dispersion Spectrum Analyzer. This unit is capable of frequency spectrum measurements over the range from 10 MHz to 63.8 GHz, in ten overlapping band settings. Sensitivity varies from -105 dbm in the lowest band, to -45 dbm in the upper band. For comparison purposes, and as a signal source of known frequency and amplitude, a Hewlett Packard Model 612A signal generator (450 MHz to 1.23 GHz) was used. Measurements were made both directly, from a

circuit similar to Figure 14.a. and from the output of a coaxial cavity, as in Figure 14.c.

Microwave power measurements were made with Hewlett Packard Model 430C and Model 431A microwave power meters, both used with thermistor mounts (Model 478A). The frequency response of the thermistor mount was 10 MHz to 10 GHz. Power measurements were made from the resonant circuit outputs.

6. Experimental Results.

A total of about 45 specimens were prepared, of which 32 were actually subjected to electrical tests. The remaining were fractured during processing and assembly of the diodes, chemically destroyed, or dropped and lost while handling. Table 3 lists the results of preliminary measurements. All contacts were pressure contacts. All measurements and experiments reported below were made at room temperature.

GaAs type	Contact Material	Diodes made	Ohmic contacts
55	In	4	1
	Sn	1	0
	In-Sn	1	0
214	In	1	0
	Sn	1	0
	Sn-Pb (Solder)	3	0
276	In	2	0
	Sn	1	0
	Al	1	0
1026	In	4	4
	Sn	2	0
	In-Sn	2	2
1137	In	2	2
	Sn	1	0
1162	In	4	0
	Sn	1	0
	None	1	0
Total	In	17	7
	Sn	7	0
	In-Sn	3	2
	Sn-Pb	3	0
	Al	1	0
	None	1	0

Table 3. - Results of Contact Evaluation.

The In-Sn contact material indicated in Table 3, is that combination described on page 30. In effect, they can probably be considered as pure indium contacts. In this case, all the ohmic contacts occurred in low resistivity, undoped GaAs, with indium as the contact material. Those diodes with ohmic contacts are listed in Table 4.

Diode	Contact	Resistance Forward	(Ohms) Back
55-3	In	25	60
1026-1	In	45	100
1026-2	In	26	75
1026-5	In-Sn	255	392
1026-6	In	*	*
1026-7	In-Sn	50	200
1026-8	In	*	*
1137-2	In	36.7	*
1137-3	In	21	*

*Not measured. Diode was destroyed before data was taken.

Table 4. Diodes with Ohmic Contacts.

All the diodes listed in Table 4 had a thickness of about 0.2 mm. The effective cross-sectional area depended on the spreading of the indium under pressure; and may generally be taken as the cross-sectional area of the GaAs specimen, which was 3 to 4 mm^2.

A wide variety of current-voltage characteristics were

displayed by the non-ohmic contacts. Most showed some type of exponential behaviour typical of semiconductors. Some showed rectifying behaviour, and other junction effects. Some examples of the various current-voltage relationships observed are shown in Figure 15.

The origin of coordinates in Figure 15.a.,b., and c., is the intersection of the arrows. The origin of coordinates is not shown in Figure 15.d. The left edge of the figure represents 20 volts. The flat portion of the trace represents zero amperes of current.

Most of the diodes, including those which did not have ohmic contacts, displayed various instabilities. In many cases, these could be traced to the junction effects; such as in Figure 15.d. In no case, were coherent oscillations, characteristic of the Gunn effect, observed. Difficulties with the sampling unit prevented the direct observance of the pulse

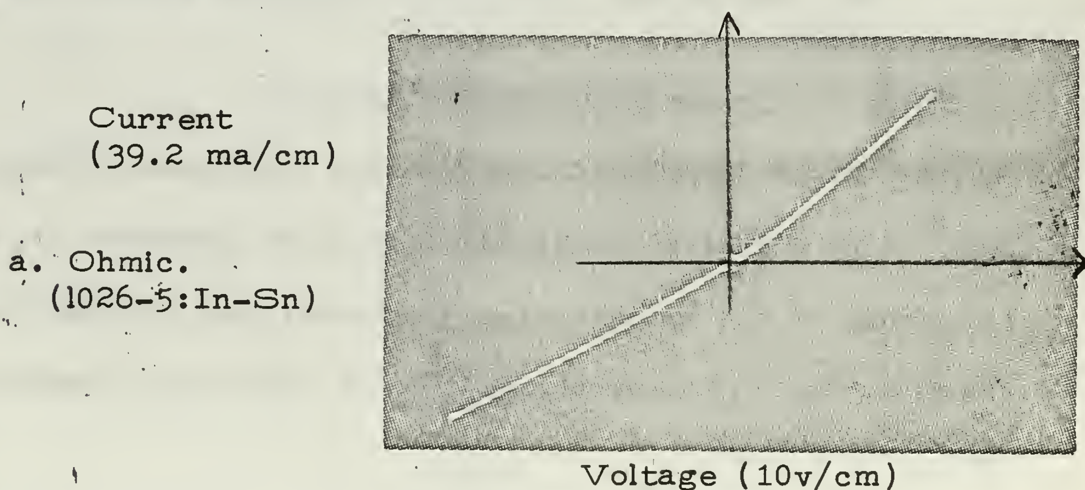

Figure 15. - Current-Voltage Characteristics observed.

Current
(0.5 ma/cm)

b. Exponential.

(1162-5:In)

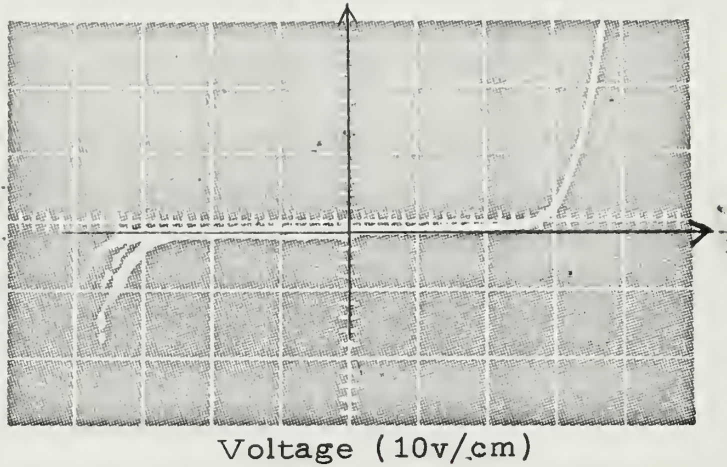

Voltage (10v/cm)

Current
(5.0 ma/cm)

c. Rectifying.

(55-5:In)

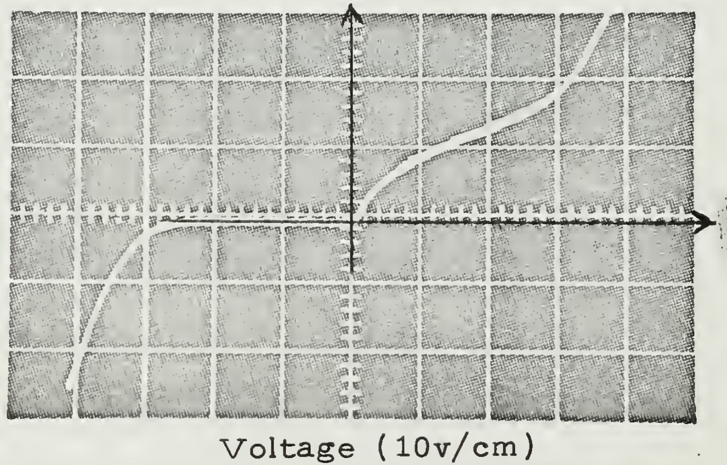

Voltage (10v/cm)

Current
(0.02 ma/cm)

d. Junction
effects.

(1162-3:In)

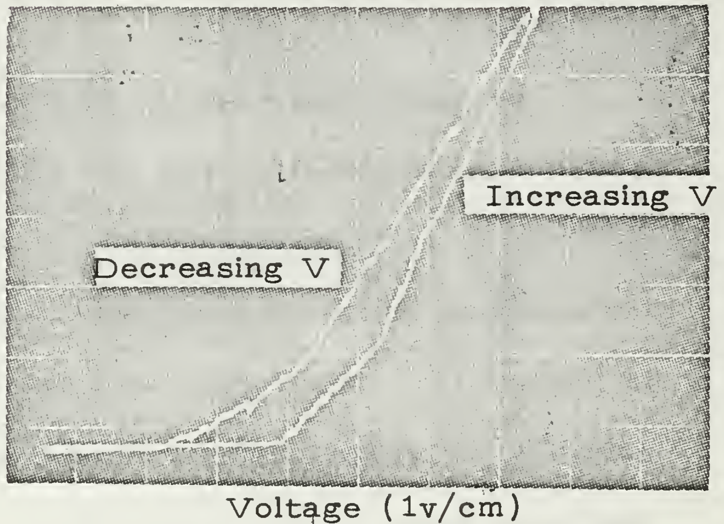

Voltage (1v/cm)

Figure 15 (continued). Current-Voltage Characteristics Observed.

output waveforms of all diodes.

Current saturation, also characteristic of the Gunn effect, was observed in several instances. Examples of this limiting are shown in Figure 16. These traces were made by a Tektronix 515A oscilloscope; hence, the band-pass limitations prevented the observance of any high frequency fluctuations which may have accompanied this limiting. The traces were made by photographing the current through the diode, resulting from repeated saw-tooth-voltage pulsing of the diode (as were the traces in Figure 15.)

Several of the diodes with non-ohmic contacts displayed a less pronounced current limiting. The result was similar to the positive voltage portion of Figure 15.c., where the portion from four to ten volts displays an increasing resistance with increasing voltage. In some cases, the successive pulse traces followed different paths in the central portion of the curve, as shown in Figure 16.b.

The pulse shape of the thyratron pulser, described in Section 5, tended to mask the effects of the pulse on the diodes. A definite disturbance in the waveform of current through one diode was observed. This disturbance is shown in Figure 17. The figure was drawn from a photograph not suitable for reproduction. The trace on the left represents the input pulse to the diode; that on the right represents the current through the diode. The two traces were intentionally

Current
(133 ma/cm)

a. Ohmic
Contacts.
(1137-2:In)

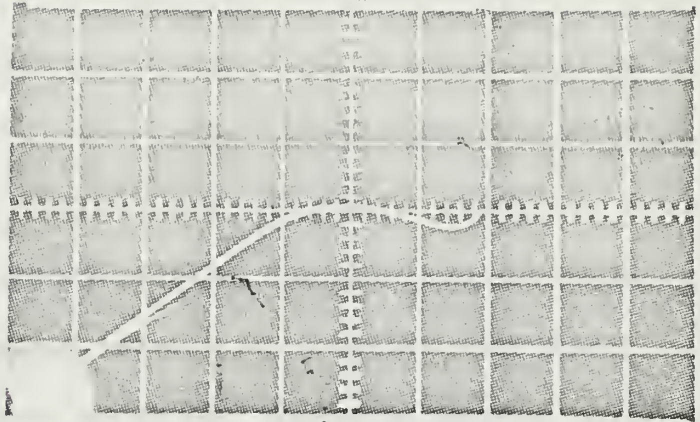

Voltage (5v/cm)

Current
(133 ma/cm)

b. Non-ohmic
Contacts.
(55-2:In)

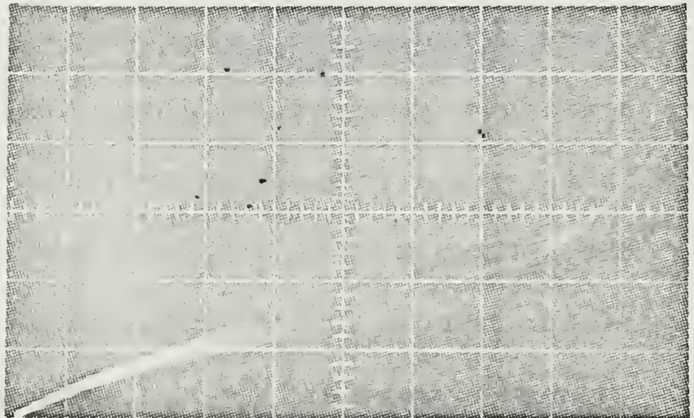

Voltage (3v/cm)

Figure 16. - Current saturation.

Input Voltage
(20v/cm)

Diode current
(33 ma/cm)

(276-2:Sn-Pb)

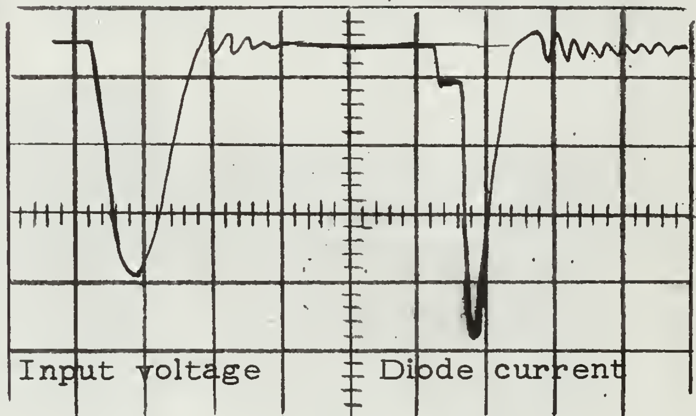

Time (200 nsec/cm)

Figure 17. - Response to Thyratron Pulser.

shifted horizontally. No delay was noticeable between pulses, with the time scale used.

Those diodes in which impact ionization apparently occurred prior to any current saturation or instability, showed a strong hysteresis effect. A typical example is shown in Figure 18. The current through the diode was limited to prevent damage of the diode. The bright spot on the upper portion of the trace indicates the limited value (225 ma). For diodes with non-ohmic contacts, in which this rapid breakdown occurred, there was a pronounced tendency to cycle around the loop when the voltage across the diode was held at the breakdown voltage, rather than a jump to the limited value of current. The loop widened upward and to the right with successive cycling. The effect did not occur when the diode was cold, would appear after the diode had been pulsed several times, and disappeared as the diode heated. Heating of the diode under this condition

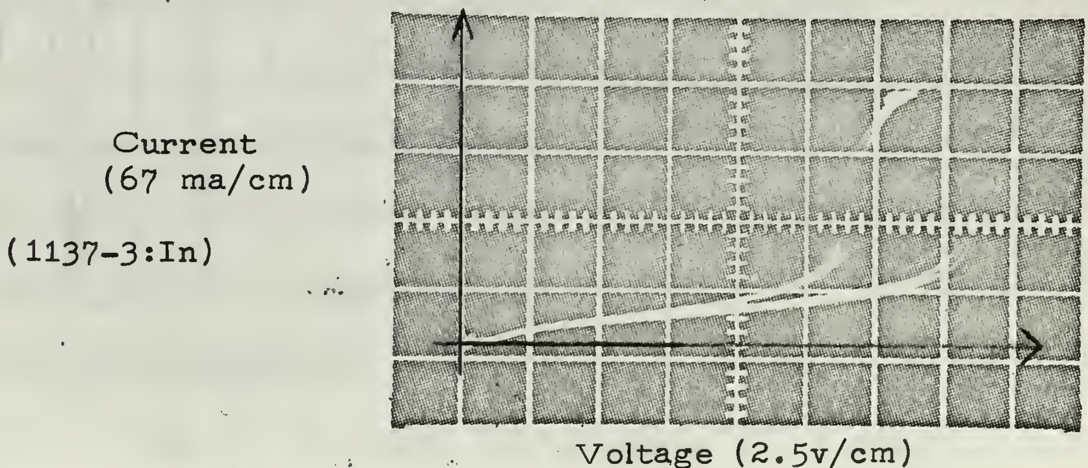

Figure 18. - Hysteresis Effect.

was very rapid, the trace showing the form of Figure 18, with the spot remaining at the limited value after a few seconds. This effect was apparently due to an oscillation, by the diode, with the current-limiting circuit of the voltage source.

The results of spectrum analysis of the output from the pulsed diodes, with the mount in Figure 8, did not reveal any discernible frequency spectrum which could definitely be attributed to the diode. In no case was a sharp spectrum observed. Any instabilities apparently had the character of broad-band noise, and could not be separated from the noise in the analyzer output.

With the spectrum analyzer connected to the high-Q coaxial cavity output, for one diode the output shown in Figure 19 was observed. The cavity was tuned to 700 MHz (one-half wavelength) as determined by the output response to an input signal from the UHF signal generator, and the cavity length. The output was intermittent and ceased after

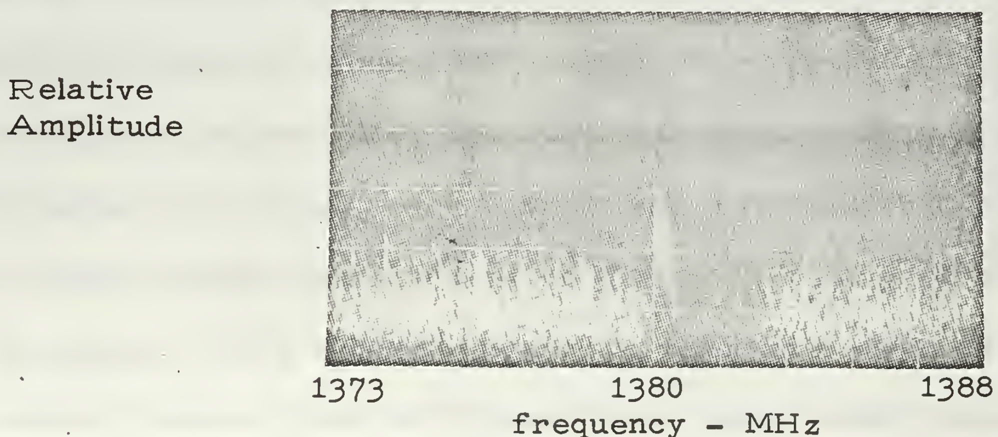

Figure 19 - Coaxial Cavity Output for Diode 1026-5:In-Sn.

about ten minutes. Subsequent examination of the diode showed it to be in several pieces. The diode was pulsed with a positive 50-volt pulse of 100 nsec duration, at a rate of 1000 pulses per second. The spectrum analyzer was at its most sensitive setting. As seen in the figure, the output is just above the noise level of the spectrum analyzer.

Cavity power measurements, using the microwave power meters, did not indicate that any significant power was being generated by the pulsed diodes. The maximum power reading obtained was 50 microwatts with diode 1026-4. This level was just above the noise in the meter. No response could be obtained by the spectrum analyzer for this output. It was apparently noise being generated by the diode.

Of the two diodes supplied by Dr. Dow of Varian Associates, diode 90G3 was tested. Preliminary tests in the mount shown in Figure 10, revealed instabilities in the diode output. The onset of instability was somewhat higher than expected, occurring at about 36 volts. Maximum instability was observed at slightly over 50 volts. The results are shown in Figure 20. The time scale is the same for both traces, which are drawn from oscilloscope photographs not suitable for reproduction. No frequency spectrum or power measurements were made. The diode was inadvertently fractured while mounting in the radar diode holder, for tests in a low-Q coaxial circuit. Tests of diode 90B7 were not conducted.

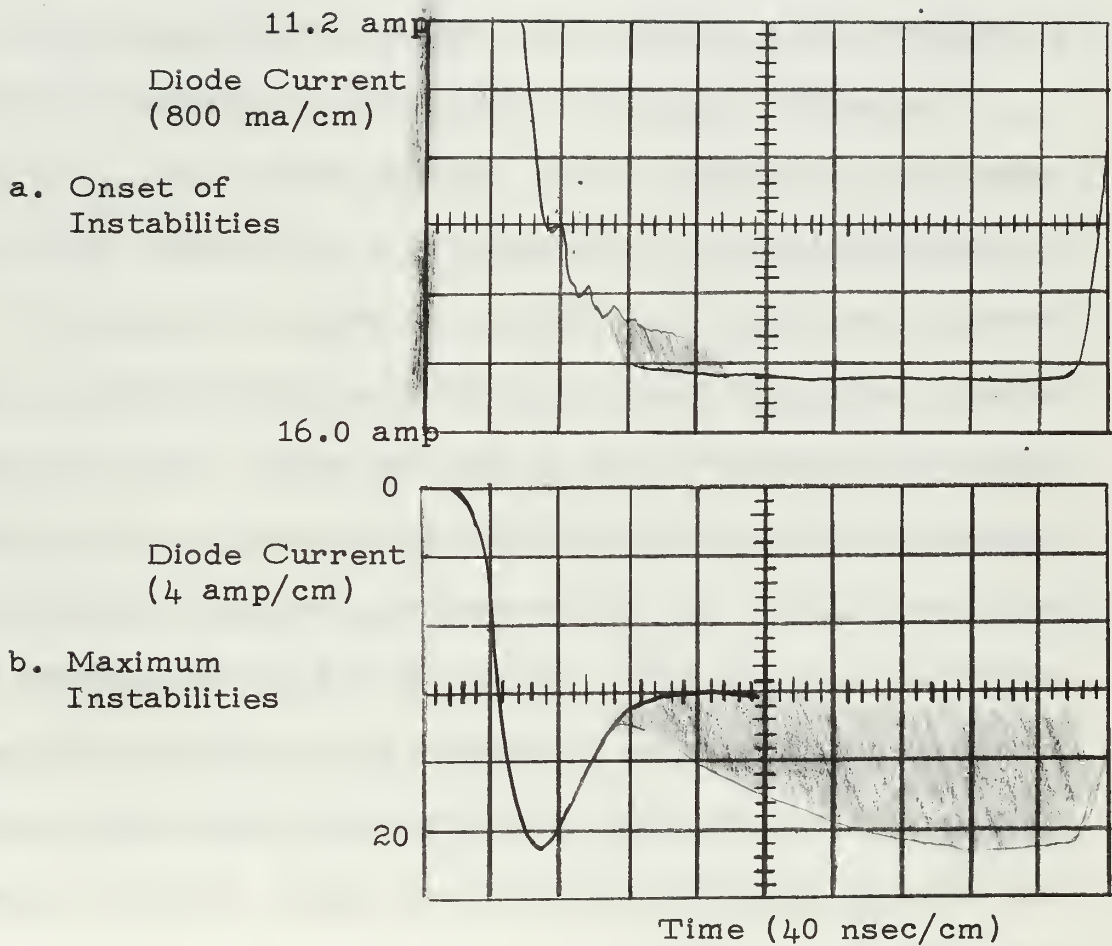

Figure 20. - Instabilities in Varian Diode 90G3.

7. Conclusions and Acknowledgements.

Gallium arsenide is not a particularly easy material with which to work. Due to its frangible nature, special techniques for preparation and handling of the bulk material are required. As with all semi-conductor materials, the properties of GaAs are a sensitive function of the amount and nature of the impurities present. Special care must be taken to prevent contamination of the material during the alloying process. Either a high vacuum, or a chemically "clean" inert atmosphere, is a necessity for alloying contacts to GaAs.

The inability to predict the nature of pressure contacts makes them undesirable for a working device. The requirement for pressure limits the thickness to a value great enough to prevent fracture of the GaAs. At best, an unsure and variable contact is made. In addition, the properties of GaAs change with pressure, due to the decreasing, with increasing pressure, of the energy difference between the levels shown in Figure 2 [7]. At high pressures, the Gunn oscillations are completely quenched [33]. Indium is the better material for pressure contacts, since it adheres to the GaAs more readily. However, it creeps under pressure, and unless special measures are taken to limit this movement, a "short circuit" is eventually produced.

Low resistivity GaAs presents electrical problems. In order to obtain the high values of electric field required in the

material for the oscillations to occur, a large current is needed. This, in turn, calls for short pulses to prevent damage to the diode. Higher resistivity material is probably better for a practical device, if enough carriers are available in the material to produce the effect. Such a device will function continuously with a DC voltage supply in place of the special pulsing requirements with lower impedance devices. Impedance matching is also less of a problem with higher impedance devices. Lowering the temperature of the device by immersing it in liquid nitrogen or some other low temperature environment, is a means of obtaining a higher impedance. This limits the usefulness, however since one of the more inviting aspects of the Gunn effect is its occurrence at room temperatures.

Although the Gunn effect is a bulk property which is much more independent of external circuit conditions than other negative resistance devices, there is some dependence. Most reports indicate frequency tuning of the diode output, over various ranges, for samples mounted in resonant cavities, by varying the resonant frequency of the cavity. The oscillations are also somewhat sensitive to the load impedance seen by the diode [18,60,87] . Frequency modulation of the output has been reported in some cases [48,61,80] .

Diode thickness limits the frequency obtainable, with material of the purity presently available. With better control of added impurities, it may be possible to trigger the domain

formation at at several points in a crystal, thus making frequency independent of sample length. Oscillations have been reported in GaAs "grown" in epitaxial layers [38,76] . Another interesting possibility for obtaining a small effective length in samples, is the surface-oriented device, where both contacts are applied to the same surface and separated by the effective length desired [45] .

Power output obtained was very low. In any event, power output will be limited by the protection necessary for preventing damage to the diode. Larger devices, with improved heat dissipation capabilities will improve this condition. Large devices will require better methods of producing extremely pure, homogeneous crystals.

Much work remains to be done before the Gunn oscillator moves from the research laboratories to the device manufacturers' inventories. That this will be done, and that the Gunn effect will fulfill its promise of an efficient, convenient source of microwave power must surely follow the efforts being made. The only question remaining is: How soon?

Many individuals were of assistance in the conduct of this project. Acknowledgement is necessary for the advice and assistance of Professor J. R. Clark and the laboratory assistants of the Department of Material Science and Chemistry, in working with the bulk GaAs. The comments and advice of Doctor D. G. Dow, of Varian Associates, Palo

Alto, California, were helpful, and his generosity in supplying two working diodes very much appreciated. Lastly, appreciation must be expressed to Professor G. L. Sackman, the advisor for this project, not only for suggesting the topic, and his advice and counsel during the conduct of the project, but also for his limitless patience during the preparation of this report.

8. Bibliography.

1. Kittel, C. Introduction to Solid State Physics, 2nd ed. John Wiley & Sons, 1956.

2. Ginzton, E. L. Microwave Measurements. McGraw-Hill, 1957.

3. Kromer, H. Proposed Negative-Mass Microwave Amplifier. Physical Review, v. 109, March, 1958: 1856.

4. Stratton, R. The Influence of interelectronic collisions on conduction and breakdown in polar crystals. Proceedings of the Royal Society, Series A, v. 246, August 19, 1958: 406-422.

5. Kromer, H. The physical principles of a negative-mass amplifier. Proceedings of the Institute of Radio Engineers, v. 47, March, 1959: 397-406.

6. Gatos, H. C. (ed.) Properties of Elemental and Compound Semi-conductors. Interscience Publishers, 1960.

7. Ehrenreich, H. Band structure and electron transport in GaAs. Phsical Review, v. 120, December 15, 1960: 1951-1963.

8. Ridley, B. K. and T. B. Watkins. The possibility of negative resistance effects in semiconductors. Proceedings of the Physical Society (of London), Part 2, v. 78, August 1, 1961: 293-304.

9. Van Velzer, H. L. Physics and Chemistry of Electronic Technology. McGraw-Hill, 1962.

10. Hilsum, C. Transferred electron amplifiers and oscillators. Proceedings of the Institute of Radio Engineers, v. 50, February, 1962: 185-189.

11. Gunn, J. B. Travelling-wave interaction between the optical modes of a polar lattice and a stream of charge carriers. Physics Letters, v. 4, April 1,1963: 194-195.

12. Ridley, B. K. and R. G. Pratt. A bulk differential negative resistance due to electron tunneling through an impurity potential barrier. Physics Letters, v. 4 May 1, 1963: 300-302.

13. Gunn, J. B. Microwave oscillations of current in III-V semiconductors. Solid State Communications, v. 1, September, 1963: 88-91.

14. Ridley, B. K. Specific negative resistance in solids. Proceedings of the Physical Society (of London), v.82, December, 1963: 954-966.

15. Ikoma, H. et al. Optical phonon effects in GaAs. Journal of the Physical Society of Japan, v. 19, January, 1964: 141-142.

16. Northrop, D. C. et al. Electrical transients in high resistivity gallium arsenide. Solid-State Electronics, v. 7, January, 1964: 17-30.

17. Dale, J. R. and M. J. Josh. Alloys for GaAs devices. Solid-State Electronics, v. 7, February, 1964: 177-181.

18. Gunn, J. B. Instabilities of current in III-V semiconductors. IBM Journal of Research and Development, v. 8, April, 1964: 141-159.

19. Kuru, I. Microwave emission from GaAs. Journal of the Physical Society of Japan, v. 19, June, 1964: 1083.

20. Matthei, W. G. Advances in solid-state microwave devices. U. S. Army Electronics Laboratories, Fort Monmouth, New Jersey. Technical report no. 2476; DDC no. AD 605923. July, 1964.

21. Mattox, D. M. Film deposition using accelerated ions. Electro-chemical Technology, v. 2, September-October 1964: 295-298.

22. Braslau, N. et al. Continuous microwave oscillations of current in GaAs. IBM Journal of Research and Development, v. 8, November, 1964: 545-546.

23. McCumber, D. E. and A. G. Chynoweth. Electrostatic instabilities in one-stream plasmas in semiconductors. Physical Review Letters, v. 13, November 30, 1964: 651-654.

24. Kroemer, H. Theory of the Gunn effect. Proceedings of the IEEE, v. 52, December, 1964: 1736.

25. Ikoma, H. Nonuniform electric field distribution in GaAs. Journal of the Physical Society of Japan, v. 19, December, 1964: 2338-2339.

26. Kroemer, H. and G. F. Day. A study of solid state microwave devices and phenomena (Research on the Gunn effect). Central Research Laboratory, Varian Associates, Palo Alto, California, Interim engineering report no. 5; DDC no. AD 462723, January, 1965.

27. Hakki, B. W. and J. C. Irvin. CW microwave oscillations in GaAs. Proceedings of the IEEE, v. 53, January, 1965: 80.

28. Woodruff, T. O. Some features of the velocity distribution of rapidly drifting electrons important in a theory of the Gunn effect (abstract).

29. Foyt, A. G. and A. L. McWhorter. Gunn effect in GaAs (abstract).

30. Day, G. F. Two bulk negative-resistance effects in high-resistivity GaAs (abstract).
Bulletin of the American Physical Society, Series II, v. 10, March, 1965: 383.

31. Quist, T. M. and A. G. Foyt. S-band GaAs Gunn effect oscillators. Proceedings of the IEEE, v. 53, March, 1965: 303-304.

32. Kroemer, H. and G. F. Day. A study of solid state microwave devices and phenomena (Research on the Gunn effect). Central Research Laboratory, Varian Associates, Palo Alto, California, Interim engineering report no. 6; DDC no. AD 462724, April, 1965.

33. Hutson, A. R. et al. Mechanism of the Gunn effect from a pressure experiment. Physical Review Letters, v. 14, April 19, 1965: 639-641.

34. Heeks, J. S. et al. Coherent high field oscillations in long samples of GaAs. Proceedings of the IEEE, v. 53, May, 1965: 554-555.

35. Ridley, B. K. The propagation of space-charge waves in a conductor exhibiting a differential negative resistance. Physics Letters, v. 16, May 15, 1965: 105-107.

36. Hakki, B. W. and S. Knight. Phenomenological aspects of CW microwave oscillations in GaAs. Solid-State Communications, v. 3, May 1965: 89-91.

37. Butcher, P. N. and W. Fawcett. Intervalley transfer of hot electrons in gallium arsenide. Physics Letters, v. 17, July 15, 1965: 216-217.

38. Hilsum, C. et al. C. W. X and K band radiation from GaAs epitaxial layers. Electronics Letters, v. 1, August, 1965: 178.

39. Allen, J. W. et al. Microwave oscillations in $GaAs_x$-P_{1-x} alloys. Applied Physics Letters, v. 7, August 15, 1965: 78-80.

40. Kroemer, H. and G. F. Day. A study of solid state microwave devices and phenomena (Research on the Gunn effect). Central Research Laboratory, Varian Associates, Palo Alto, California, Technical report no. AFAL-TR-65-238, September, 1965.

41. Carroll, J. E. Domain stability in the Gunn effect. Electronics Letters, v. 1, September, 1965: 189-190.

42. Hilsum, C. A simple analysis of transferred electron oscillators. British Journal of Applied Physics, v. 16, September, 1965: 1401-1403.

43. Thim, H. W. et al. Microwave amplification in a DC-biased bulk semiconductor. Applied Physics Letters, v. 7, September 15, 1965: 167-168.

44. Kroemer, H. External Negative conductance of a semiconductor with negative differential mobility. Proceedings of the IEEE, v. 53, September, 1965: 1246.

45. Foxell, C. A. P. et al. Surface-oriented Gunn-effect oscillator. Electronics Letters, v. 1, October, 1965: 217.

46. Carroll, J. E. Domain Stability in the Gunn Effect. Services Electronics Research Laboratory (SERL) Technical Journal, v. 15, October, 1965: 22.1-22.4 (Same as 41.)

47. Kennedy, W. K. Jr. Variation of the Gunn effect by magnetic field. 1639-1640.

48. Kuru, I. Frequency modulation of the Gunn oscillator. 1642-164 .

49. Fleming, P. L. Synchronization of microwave oscillations in GaAs. 1665-1666.

Proceedings of the IEEE, v. 53, October, 1965.

50. Wadhwa, R. P. Transit time effects in gaseous and solid-state devices. 1738-1739.

51. Munson, H. B. Jr. Frequency control of pulsed GaAs Gunn effect diodes by injection locking. 1781-1782.

52. Shaskus, A. J. and M. P. Shaw. Current instabilities in gallium arsenide. 1804-1805.

Proceedings of the IEEE, v. 53, November, 1965.

53. Kuru, I. A possibility of the collective phonon wave in n-GaAs. Central Research Laboratory, Tokyo Shibaura Electric Company, Limited, Kawasaki, Japan, unpublished report, November, 1965.

54. Sterzer, F. Progress in solid-state microwave power sources. IEEE Transactions on Microwave Theory and Techniques, v. MTT-13, November, 1965: 768-772.

55. Day, G. F. et al. A study of solid state devices and phenomena (The Gunn effect: New applications and materials). Central Research Laboratory, Varian Associates, Palo Alto, California, Interim technical report no. 1; Varian engineering report no. 336-1Q, December, 1965.

56. Hervouet, C. et al. Current oscillations in GaAs under acoustic amplification conditions. Solid State Communications, v. 3, December, 1965: 413-415.

57. Butcher, P. N. and C. Hilsum. Domain configuration in transferred electron oscillators. Electronics Letters, v. 1, December, 1965: 286.

58. Butcher, P. N. and W. Fawcett. The intervelley transfer mechanism of negative resistivity in bulk semiconductors. Proceedings of the Physical Society of London, v. 86, December, 1965: 1205-1219.

59. Akasaki, I. and T. Hara. Temperature dependence of electron mobility in GaAs. Journal of the Physical Society of Japan, v. 20, December, 1965: 2292.

60. Robson, P. N. and S. M. Mahrous. Some aspects of Gunn effect oscillators. 345-352.

61. Heeks, J. S. et al. The mechanism and device applications of high field instabilities in gallium arsenide. 377-387.

The Radio and Electronics Engineer, v. 30, December, 1965.

62. McCumber, D. E. and A. G. Chynoweth, Theory of negative-conductance amplification and of Gunn instabilities in "two-valley" semiconductors. 4-21.

63. Conwell, E. M. and M. O. Vasell. High-field distribution function in GaAs. 22-27.

64. Kroemer, H. Nonlinear space-charge domain dynamics in a semiconductor with negative differential mobility. 27-40.

65. Ridley, B. K. The inhibition of negative resistance dipole waves and domains in n-GaAs. 41-43.

66. Engelmann, R. W. H. and C. F. Quate. Linear, or "small-signal", theory for the Gunn effect. 44-52.

67. Sumi, C. M. Current oscillations by coherent excitation of optical phonons. 53-57.

68. Vural, B. and S. Bloom. Streaming instabilities in solids and the role of collisions. 57-63.

69. Shyam, M. et al. Effect of variation of energy minima separation in Gunn oscillations. 63-67.

70. Heeks, J. S. Some properties of the moving high-field domain in Gunn effect devices. 68-79.

71. Foyt, A. G. and A. L. McWhorter. The Gunn effect in polar semiconductors. 79-87.

72. Day, G. F. Microwave oscillations in high-resistivity GaAs. 88-94.

73. Hakki, B. W. and S. Knight. Microwave phenomena in bulk GaAs. 94-105.

74. Dow, D. G. et al. High-peak-power gallium arsenide oscillators. 105-110.

75. Thim, H. W. and M. R. Barber. Microwave amplification in a GaAs bulk semiconductor. 110-114.

76. Hasty, T. E. et al. Microwave oscillations in epitaxial layers of GaAs. 114-117.

77. Carroll, J. E. Nonisothermal waves on charge carrier streams. 187-189.

78. Copeland, J. A. Electrostatic domains in two-valley semiconductors. 189-192.

79. Butcher, P. N. et al. The dependence of threshold field on intervalley separation in transferred electron oscillators. 192-193.

80. Bott, I. B. et al. Amplitude and frequency modulation of transferred electron microwave generators. 193-194.

81. Bosch, B. G. and H. Pollmann. Frequency synchronization of Gunn effect oscillators. 194-196.

82. Yamashita, A. and R. Nii. A mechanism of current saturation in n-type GaAs. 196-197.

83. Hakki, B. W. et al. Phase-locked GaAs CW microwave oscillators. 197-199.

84. Foyt, A. G. and T. M. Quist. Bulk GaAs microwave amplifiers. 199-200.

85. Hayashi, T. and M. Uenohara. Evaluation of metal-semiconductor contacts in bulk GaAs oscillators by the photovoltaic effect. 200-201.

86. Lawlay, K. L. et al. N-type GaAs for CW microwave devices. 201-202.

<u>IEEE Transactions on Electron Devices,</u> v. ED-13, January, 1966 (Special issue on semiconductor bulk-effect and transit-time devices).

87. Matino, H. and I. Kuru. Reactance of GaAs bulk oscillator. 291-292.

88. Hakki, B. W. GaAs post-threshold microwave amplifier, mixer, and oscillator. 299-300.

89. Suematsu, Y. and Y. Nishimura. Wave theory of the negative resistance element due to Gunn effect. 322-324.

<u>Proceedings of the IEEE,</u> v. 54, February, 1966.

90. Mao, S. and R. A. Pucel. Gunn oscillators in the 5-20 GHz range. <u>Proceedings of the IEEE,</u> v. 54, March, 1966: 414-415.

91. Draysey, D. W. et al. Noise performance of Gunn microwave generators in X and J band. Electronics Letters, v. 2, March 1966: 125-126.

92. Dow, D. G. Personal discussion, March 31, 1966.

93. Hilsum, C. Negative resistance due to mixed scattering. 576-577.

94. Volkov, A. F. Steady-state waves in semi-conductors with negative differential resistance. 598-600. Physics Letters, v. 20, April 1, 1966.

95. Kennedy, W. K. Jr. Power generation in GaAs at frequencies far in excess of the intrinsic Gunn frequency. Proceedings of the IEEE, v. 54, April, 1966: 710.

INITIAL DISTRIBUTION LIST

		No. Copies
1.	Defense Documentation Center Cameron Station Alexandria, Virginia 22314	20
2.	Library U. S. Naval Postgraduate School Monterey, California 93940	2
3.	Commandant of the Marine Corps (Code AO3C) Headquarters, U. S. Marine Corps. Washington, D. C. 22214	1
4.	Professor G. L. Sackman Department of Electrical Engineering U. S. Naval Postgraduate School Monterey, California 93940	2
5.	Major A. A. Slepicka, USMC Marine Corps Schools Quantico, Virginia	1
6.	Dr. D. G. Dow Varian Associates 611 Hansen Way Palo Alto, California	1

DOCUMENT CONTROL DATA - R&D

(Security classification of title, body of abstract and indexing annotation must be entered when the overall report is classified)

1. ORIGINATING ACTIVITY (Corporate author)	2a. REPORT SECURITY CLASSIFICATION
U. S. Naval Postgraduate School, Monterey, California 93940	UNCLASSIFIED
	2b. GROUP

3. REPORT TITLE
INVESTIGATION OF THE GUNN EFFECT IN GALLIUM ARSENIDE

4. DESCRIPTIVE NOTES (Type of report and inclusive dates)
Thesis (MS)

5. AUTHOR(S) (Last name, first name, initial)
SLEPICKA, Alois A., Major, U. S. Marine Corps

6. REPORT DATE	7a. TOTAL NO. OF PAGES	7b. NO. OF REFS
May 1966	74	95

8a. CONTRACT OR GRANT NO.	9a. ORIGINATOR'S REPORT NUMBER(S)
b. PROJECT NO.	
c.	9b. OTHER REPORT NO(S) (Any other numbers that may be assigned this report)
d.	

10. AVAILABILITY/LIMITATION NOTICES

[illegible]

11. SUPPLEMENTARY NOTES	12. SPONSORING MILITARY ACTIVITY
	U.S. Marine Corps

13. ABSTRACT

The Gunn effect is a recently (1963) observed phenomenon in the electrical properties of certain compound semiconductors. It is characterized by a sudden onset of oscillations in current through the material when a critical value of electric field is exceeded. The oscillations are not greatly affected by external circuit conditions, are at microwave frequencies, and occur as a bulk property at room temperature in gallium arsenide and certain other materials with the proper conduction band structure. The intervalley transfer of electrons in the conduction band from a lower energy high mobility sub-band, to a higher energy low mobility sub-band with the application of an increasing electric field gives rise to a negative differential resistance in the material. It is this mechanism which is accepted as the cause of the instabilities. A brief theoretical explanation is given. The preparation of samples of gallium arsenide is described and discussed. Sample mounting is described, and the results of various tests reported. The value of the effect lies in the ability to directly convert pulse or DC power into microwave power at usable levels and at reasonable efficiencies.

14. KEY WORDS	LINK A		LINK B		LINK C	
	ROLE	WT	ROLE	WT	ROLE	WT
Gunn effect						
Semiconductor						
Solid-state						
Microwave						
Electrical instability						
Gallium arsenide						
Semiconductor oscillations						
Solid-state power source						

INSTRUCTIONS

1. **ORIGINATING ACTIVITY:** Enter the name and address of the contractor, subcontractor, grantee, Department of Defense activity or other organization *(corporate author)* issuing the report.

2a. **REPORT SECURITY CLASSIFICATION:** Enter the overall security classification of the report. Indicate whether "Restricted Data" is included. Marking is to be in accordance with appropriate security regulations.

2b. **GROUP:** Automatic downgrading is specified in DoD Directive 5200.10 and Armed Forces Industrial Manual. Enter the group number. Also, when applicable, show that optional markings have been used for Group 3 and Group 4 as authorized.

3. **REPORT TITLE:** Enter the complete report title in all capital letters. Titles in all cases should be unclassified. If a meaningful title cannot be selected without classification, show title classification in all capitals in parenthesis immediately following the title.

4. **DESCRIPTIVE NOTES:** If appropriate, enter the type of report, e.g., interim, progress, summary, annual, or final. Give the inclusive dates when a specific reporting period is covered.

5. **AUTHOR(S):** Enter the name(s) of author(s) as shown on or in the report. Enter last name, first name, middle initial. If military, show rank and branch of service. The name of the principal author is an absolute minimum requirement.

6. **REPORT DATE:** Enter the date of the report as day, month, year; or month, year. If more than one date appears on the report, use date of publication.

7a. **TOTAL NUMBER OF PAGES:** The total page count should follow normal pagination procedures, i.e., enter the number of pages containing information.

7b. **NUMBER OF REFERENCES:** Enter the total number of references cited in the report.

8a. **CONTRACT OR GRANT NUMBER:** If appropriate, enter the applicable number of the contract or grant under which the report was written.

8b, 8c, & 8d. **PROJECT NUMBER:** Enter the appropriate military department identification, such as project number, subproject number, system numbers, task number, etc.

9a. **ORIGINATOR'S REPORT NUMBER(S):** Enter the official report number by which the document will be identified and controlled by the originating activity. This number must be unique to this report.

9b. **OTHER REPORT NUMBER(S):** If the report has been assigned any other report numbers *(either by the originator or by the sponsor)*, also enter this number(s).

10. **AVAILABILITY/LIMITATION NOTICES:** Enter any limitations on further dissemination of the report, other than those imposed by security classification, using standard statements such as:

(1) "Qualified requesters may obtain copies of this report from DDC."

(2) "Foreign announcement and dissemination of this report by DDC is not authorized."

(3) "U. S. Government agencies may obtain copies of this report directly from DDC. Other qualified DDC users shall request through
________________________."

(4) "U. S. military agencies may obtain copies of this report directly from DDC. Other qualified users shall request through
________________________."

(5) "All distribution of this report is controlled. Qualified DDC users shall request through
________________________."

If the report has been furnished to the Office of Technical Services, Department of Commerce, for sale to the public, indicate this fact and enter the price, if known.

11. **SUPPLEMENTARY NOTES:** Use for additional explanatory notes.

12. **SPONSORING MILITARY ACTIVITY:** Enter the name of the departmental project office or laboratory sponsoring *(paying for)* the research and development. Include address.

13. **ABSTRACT:** Enter an abstract giving a brief and factual summary of the document indicative of the report, even though it may also appear elsewhere in the body of the technical report. If additional space is required, a continuation sheet shall be attached.

It is highly desirable that the abstract of classified reports be unclassified. Each paragraph of the abstract shall end with an indication of the military security classification of the information in the paragraph, represented as *(TS), (S), (C), or (U)*.

There is no limitation on the length of the abstract. However, the suggested length is from 150 to 225 words.

14. **KEY WORDS:** Key words are technically meaningful terms or short phrases that characterize a report and may be used as index entries for cataloging the report. Key words must be selected so that no security classification is required. Identifiers, such as equipment model designation, trade name, military project code name, geographic location, may be used as key words but will be followed by an indication of technical context. The assignment of links, roles, and weights is optional.

DD FORM 1 JAN 64 1473 (BACK)

22 MAR 67
29 AUG 67
16 APR 76

BINDERY
15293
15837
23478

Thesis
S5707
c.1
Slepicka
Investigation of the Gunn effect in gallium arsenide.
68656
22 MAR 67
29 AUG 67
16 APR 76

BINDERY
15293
15837
23478

Thesis
S5707
c.1
Slepicka
Investigation of the Gunn effect in gallium arsenide.
68656

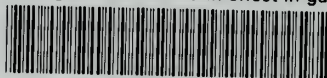
thesS5707
Investigation of the Gunn effect in gall
3 2768 002 01152 0
DUDLEY KNOX LIBRARY